8-1-2013

Numerical Modeling of Heat Pipe Radiator and Fin Size Optimization for Low and No Gravity Environments

Virginia Ruth Bieger
University of Nevada, Las Vegas, biegerv@hotmail.com

NUMERICAL MODELING OF HEAT PIPE RADIATOR AND FIN SIZE OPTIMIZATION FOR LOW AND NO GRAVITY ENVIRONMENTS

By

Virginia R Bieger

Bachelor of Science in Chemical Engineering
Louisiana Tech University
2002

A thesis submitted in partial fulfillment
of the requirements for the

Master of Science in Engineering - Mechanical Engineering

Department of Mechanical Engineering
College of Engineering
The Graduate College

University of Nevada, Las Vegas
August 2013

THE GRADUATE COLLEGE

We recommend the thesis prepared under our supervision by

Virginia Bieger

entitled

Numerical Modeling of Heat Pipe Radiator and Fin Size Optimization for Low and No Gravity Environments

is approved in partial fulfillment of the requirements for the degree of

Master of Science in Engineering - Mechanical Engineering

Department of Mechanical Engineering

Yitung Chen, Ph.D., Committee Chair

Robert Boehm, Ph.D., Committee Member

Hui Zhao, Ph.D., Committee Member

Jian Ma, Ph.D., Committee Member

Yingtao Jiang, Ph.D., Graduate College Representative

Kathryn Hausbeck Korgan, Ph.D., Interim Dean of the Graduate College

August 2013

ABSTRACT

NUMERICAL MODELING OF HEAT PIPE RADIATOR
AND FIN SIZE OPTIMIZATION FOR
LOW AND NO GRAVITY
ENVIRONMENTS
by

Virginia Bieger

Dr. Yi-Tung Chen, Examination Committee Chair
Professor of Mechanical Engineering
University of Nevada, Las Vegas

A heat-pipe radiator element has been designed and modeled to study the efficiency of heat transfer for low and no gravity environments, like in lunar environments. The advantages of using heat pipe includes the significant weight reducing and heat transfer efficiency. The heat transfer can be enhanced by the use of condenser sections with attached fins.

A series of various geometries of solid fins and heat pipes with and without fins were modeled using FLUENT®. This was done to determine the validity of using a heat pipe in lieu of a solid fin projection. A heat pipe had a 25 mm outer diameter, 23 mm inner diameter, 25 mm wide fin. The heat pipe with fin was 300 mm in length. Using the power output per unit area and power output per unit mass, to verify that a design heat pipe was the best selection for a lunar radiator system. Then, heat pipes with various fin widths were modeled using FLUENT® and their power outputs were analyzed as a function of radiation surface area and mass.

The parametric study returned the expected results that the heat pipe provided the highest power output for both the mass and radiation area. The fin width study was

used to determine the fin size that provided the most power output per unit mass. This showed an optimum fin width of 12.5 mm.

ACKNOWLEDGEMENTS

I would like to thank my thesis advisor, Dr. Jian Ma, for his help and guidance through this process. His willingness to answer questions and help point me in the right direction was invaluable. I would also like to thank my committee for all their comments and direction in my thesis work. I am indebted to my committee chair, Dr. Yi-Tung Chen, for his direction and counsel in making this thesis possible. Finally, all of this would not have been possible without the support of my husband, David, and my two children, Leigh Anne and Tucker. Their understanding and encouragement was instrumental in accomplishing this goal.

TABLE OF CONTENTS

LIST OF TABLES

LIST OF FIGURES

Chapter 1

Introduction

The ability to dissipate heat from a source to the external environment is necessary so that systems that create energy in the form of heat can operate. This heat dissipation, or heat transfer, can be accomplished through three fundamental methods: convection, conduction, or radiation. On the Earth's surface conduction and convection are the primary forms of heat transfer. Convection is transfer in a gas or liquid by the circulation of currents from one region to another. This type of heat transfer is typically used for cooling when large amounts of heat need to be removed due to the efficiency of heat transfer that can be accomplished. Conduction utilizes the direct contact between two surfaces to move heat from an area of higher temperature to an area of lower temperature. This is commonplace in all heat exchangers as conduction heat transfer is applicable to the walls of a heat exchanger. Radiation is often the negligible on the Earth's surface as it is relatively small as compared to conductive and convective heat transfer rates. This type of heat transfer is only a major factor in areas where conduction and convection are not possible or plausible. This is the case in areas where a vacuum exists such as outer space.

1.1 Overview of Extraterrestrial Radiator Design

Exploration to outer space or other planets like Mars or Moon with low gravity for long duration requires active thermal control system. Radiator or radiator systems are the essential component, which directly reject heat transferred from thermal control system to outer space by radiation heat transfer alone. Without the surrounding atmosphere at outer space, the extraterrestrial radiator system cannot rely on the terrestrial heat transfer

mechanism, like convection or combined with radiation to dissipate heat to its surrounding environment. Radiator systems for space systems also pose the challenge of needing to be lightweight and relatively compact due to transport. Since a radiator can be up to fifty percent of the total weight of a system (Brandhorst & Rodiek, 2006), there is an ever present necessity to continually redesign radiators using the most modern tools to decrease the size and weight of the radiator while maintaining or increasing the heat transfer rate and efficiency of the system.

Radiator system design consists of the design of radiator itself and overall system design including supporting structure and shading technologies. On the area of radiator device design, various areas are under study, like materials, heat pipe design, wick material in heat pipe, fin design and optimization etc. On the overall system design, the lightweight supporting structure and radiator shade geometry play an important role for the system. The lightweight supporting structure with simplicity is preferable. In addition, radiator shades with highly reflective surface can block the heat striking the radiator from lunar surface or sun, in which case the sink temperature surrounding radiator is reduced. As a result, it allows radiator to reject heat more efficiently.

The materials of design that are considered include the original materials of construction and fin material. Material with characteristics of lightweight, higher thermal conductivity, chemical inertness are attractive to reduce overall system weight and space area. The materials of construction impose the greatest constraints of system design. This material will be the primary means of heat transfer as well as the majority of the weight of the system. Because of this, the selection of the material the system will be made of is imperative to reduction of system weight and thus area.

There are three standard wick designs, slab wicks, arterial wicks, and grooved wicks. Each design has its strengths and weaknesses. The selection of design is based on operating fluid and overall system design parameters. The selection of the wicking material goes with the selection of the working fluid as any chemical interaction between the two can affect the performance of the radiator system.

Fin design is another key component in radiator system. The selection begins with a solid fin or a heat pipe fin. From there, fin geometry and how the fin attaches to the system must be addressed. For space radiator systems the majority of designs focus on heat pipe radiator fins of various geometries. Geometry selection is based upon the required heat transfer area and weight constraints.

The overall design of extraterrestrial radiator systems is scarce in literature. Some concept design can be referred in reference (Mattick & Hertzberg, 1985 and Brandhorst & Rodiek, 2006). These designs, liquid droplet radiator and liquid sheet radiator, provide a significant increase in heat transfer capability of the radiator system over the traditional heat pipe design. These conceptual designs have not yet to be fully verified and field-tested. The majority of the research uses the heat pipe system that has been around for the last 60 years.

Heat pipe integrated with fin is a promising technology to enhance the efficiency of radiator as well as reduce significantly mass of system. Heat pipes use a hollow centered pipe or other geometry with an internal working fluid to transfer heat from a thermal control system to the ambient atmosphere. This can be accomplished using one phase, typically liquid, or two phases, liquid and vapor. In the later system the latent heat of vaporization is used to remove heat from the thermal control system at the evaporator section while the

heat of condensation is utilized to transfer the heat to the surroundings in the condenser section. The use of a wick is necessary to transport the condensed liquid from the condenser back to the evaporator due to the lack of gravity. By integrating the heat pipe with the fin, the weight of the radiator can be reduced.

Optimization is the final stage of design. Every aspect of the system needs to be optimized. The majority of optimization has been done on specific portions of the system such as fin shape or heat transfer area. However, for specific designs, computer programs like ANSYS FLUENT® are used for the optimization of the entire system.

1.2 Methodology

The goal of this research is to investigate current status on space radiator systems for low and no gravity environments with new materials and technologies and using this information to design a radiator system for space systems. Various space environments are taken into consideration: deep space, lunar surface, and near earth orbit. To study these parameters, designs for the spacecraft, satellites, the international space station, and the Mars rover/pathfinder are looked into as well as conceptual designs not yet flight-tested. The parameters from the literature reviewed are compared to provide options and insight into each.

Based on the parameters of the theoretical calculations a schematic of a portion of the radiator system will be analyzed using ANSYS FLUENT®. This will include the design and analysis of the basic shapes of the component being analyzed. Using the basic components more complex assemblies can then be created and tested. The culmination of

this analysis will be able to test the component, in its entirety, to determine the radiation load and heat transfer gradient.

The basic design for a heat pipe was selected based on a literature survey. This design was recreated in FLUENT® using measurements provided by Albert Juhasz (Juhasz, 1998). This design was then meshed using four distinctly different size meshes. These mesh sizes ranged from very coarse to very fine. The temperatures at five equally spaced points on the heat pipe were calculated. These values were then analyzed to determine when the change in mesh size no longer affected the temperature gradient along the heat pipe.

The wick structure of the heat pipe was not to be considered in the design of the heat pipe structure. For this reason it was necessary to create a boundary condition profile to simulate the performance of the wick structure. Two papers, "Performance Analysis of a Liquid Metal Heat Pipe Space Shuttle Experiment" (Dickenson, 1996) and "High temperature heat pipe experiments aboard the space shuttle" (Woloshun, 1993) that analyzed the wick performance of heat pipes in space environments were studied. The temperature data for the wick structure along the heat pipe was plotted using Excel and a trend line fitted to the data. The equations of the trend lines were both considered and the equation with the lesser variance selected to approximate the wick effects in the heat pipe structure.

Once a general design was selected, was to benchmark the design. The benchmark design used an Air Force Institute of Technology Thesis "Performance Analysis of a Liquid Metal Heat Pipe Space Shuttle Experiment." (Dickenson, 1996) The design parameters of the laboratory tested heat pipe were input into FLUENT® to create a replica in the program.

From here a mesh was applied to the system and a profile representation of the wick performance was added. Outside the wick conditions, the same boundary conditions were input into FLUENT® and the simulation run to convergence. The results were then compared to the flight test data.

After the benchmark was completed, the selected design parameters were input into FLUENT® to create a three-dimensional model of various geometric shaped solid fins and various forms of the selected the heat pipe. This design was meshed using the constraints of the mesh independent study. The boundary conditions were input based on the selected material and working fluid as well as ambient conditions. FLUENT® was run until the model reached convergence. This procedure was followed for each of the designs being considered.

1.3 Results

The parametric study returned the expected results that the heat pipe provided the highest power output for both the mass and radiation surface area. The results of this study showed that the heat pipe with an integrated fin outperformed the other geometries in both power output per unit volume and power output per unit mass. This design was also the most efficient at 82%, twice that of the highest solid geometry components.

The fin width study was used to determine the fin size that provided the most power output per unit mass, power per unit area, and efficiency. The heat pipe with fin ratio 0.25 had the highest power per unit area and efficiency. However, the heat pipe with the 0.5 ratio fin had the best power output per unit mass. This power per unit mass was determined to be the deciding factor since the power per unit area values varied by less than 100 and

the efficiency of both designs was exceedingly high, the design with a better power per mass ratio was selected. This showed an optimum fin width of 12.5 mm.

Chapter 2

Literature Review

2.1 Overall Design of Radiator

2.1.1 Spacecraft Applications with no Gravity

A liquid droplet radiator (LDR) system was proposed as a possible design for a low or no gravity radiator system. This system uses sub-millimeter sized droplets of fluid generated, passed through space via generators and collectors, collected and recirculated back to a heat source. Multiple configurations of the LDR have been studied. Geometries include rectangular and triangular. These are considered the most viable and thus have been more extensively studied. Other optional geometries include spiral, enclosed disk, annular, and magnetic geometries, which also viable but not as well studied.

The LDR concept was conceived in 1978 (Pfeiffer, 1989). As shown in Figure 1 the LDR operates by spraying an array of droplet streams from a droplet generator, which form a sheet like geometry. Though similar to the liquid sheet radiator the thickness of the LDR array is much less than a regular sheet (Mattick & Hertzberg, 1985). The droplets transfer heat as they travel from the generator to the collector. Since the droplets have a large relative surface area the heat transfer rate would be extremely high (Mattick & Hertzberg, 1985). The droplets converge at a collector and the fluid is pressurized via a pump and recirculated to the heat source. The droplet stream would be shielded from the environment using two sheets of protective material.

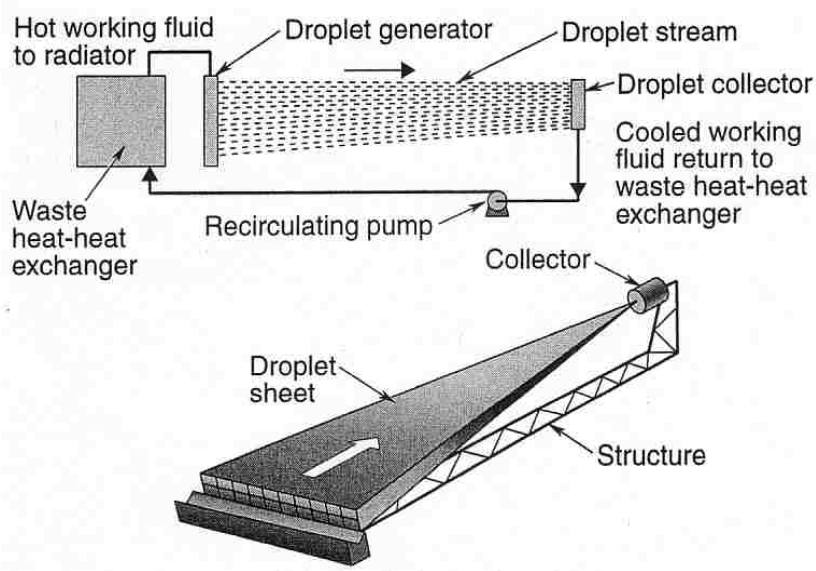

Figure 1. Schematic drawing of single pass liquid droplet radiator (LDR). (Nelson, 2007)

Benefits of the LDR system are: it can handle large quantities of heat, is significantly lighter in weight than the traditional radiator systems, maintains low deviation of droplets from stream, and in linear configuration loss of one radiator does not mean loss of the entire system. Drawbacks to this design are hard to overcome, as they are fundamental. This design is innately hard to run laboratory tests of certain critical aspects such as: generator start-up and shutdown performance, generator surface wetting, droplet collector operation, and observing backflow issues (Mattick & Hertzberg, 1985). This is due to the need for this system to operate in a low or no gravity environment for testing. Another area of concern is the number of moving parts and the effect of space debris and lunar dust on the performance. This design is primarily conceptual. There has been a minimal amount of research published as to the actual testing of this design.

2.1.2 Inhabited lunar bases with less gravity

Several concepts for newer radiator designs could be found in literatures for inhabited lunar bases. Two of these designs use liquid to directly transfer heat from the system to the environment. The liquid sheet radiator (LSR) operates as a constant temperature radiator. It uses silicon oils and the like as the working fluid. The radiator system uses the same operating fluid throughout the system. LSR design has two geometries, triangular and spherical, that can be considered feasible for design (Brandhorst & Rodiek, 2006).

The LRS operates by spraying the operating liquid through a rectangular slot as shown in Figure 2. Due to the lack of gravity along with the fluid surface tension the sheet will merge into a point, thus forming a triangular configuration. The fluid sheet would be between two sheets of protective material to prevent external debris from interrupting the sheet. For the spherical geometry, the working fluid would be sprayed upward and travels down the sides of the encapsulating sphere. The thin sheet, having a large surface area, would effectively radiate heat into space. The fluid would then be collected in the bottom for redistribution (Brandhorst & Rodiek, 2006).

Figure 2. Schematic drawing of multiple pass liquid sheet radiator (LSR). (Tagliafico and Fossa, 1999)

This design is fairly lightweight for the required area needed at an estimated 1.5 kg/m^2 (Brandhorst & Rodiek, 2006). However, this design has some larger issues to overcome. The triangular design is not stable in widths over one meter and must operate in near vacuum environments as to not affect the sheet surface tension, sheet velocity, and sheet geometry (Brandhorst & Rodiek, 2006).

The LSR design is only in the beginning stages of research. Though theoretically feasible, there is much work needed to design an operational prototype. Fluid flow dynamics of the operating fluid as well as the liquid sheet and encapsulating material interaction would need to be extensively studied. System constraints of the LSR design, especially between the working fluid volumes and attainable radiating surfaces, have shown that this design is not particularly promising compared to existing radiator systems at the present time (Tagliafico and Fossa, 1999).

2.1.3 Dual Environment System

Most of the operational radiator designs consist of traditional heat pipe radiators. This design has been in use since the 1960's and is effective in purely radiative environments. Heat pipe radiators can be found in outer space on the International Space Station (ISS) and low gravity environments such as on Mars Pathfinder and Rover. These systems included single-phase systems such as the Mars Pathfinder and Rover (Ganapathi, et al., 2003), and two-phase systems like those found on the ISS.

A typical heat pipe consists of a sealed pipe or tube made of a material with high thermal conductivity. A vacuum pump is used to remove all air from the empty heat pipe, and then the pipe is filled with a fraction of a percent by volume of working fluid chosen to match the operating temperature. Due to the partial vacuum that is near or below the vapor pressure of the fluid, some of the fluid will be in the liquid phase and some will be in the gas phase. The use of a vacuum eliminates the need for the working gas to diffuse through any other gas and so the bulk transfer of the vapor to the cold end of the heat pipe is at the speed of the moving molecules (Faghri, 1995). Inside the pipe a wick is used to exert capillary pressure on the liquid phase of the working fluid as it condenses. This is typically metal mesh or a series of grooves that runs parallel along the length of the pipe. The wick is used to remove condensed liquid back to the heated end of the system in low and no gravity environments. Possible configurations of heat pipes working in a system are shown in Figures 3 and 4. Both figures show multiple heat pipes with integrated fins and their relation to one another.

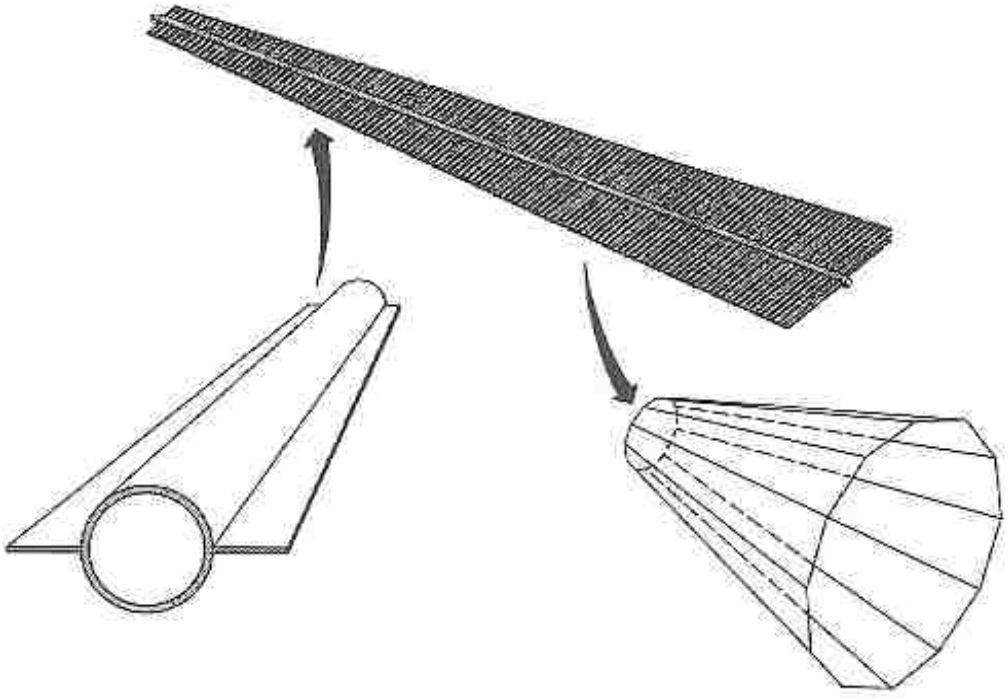

Figure 3. Diagram of heat pipe with integrated fin and possible configurations. (Jushaz, 1998)

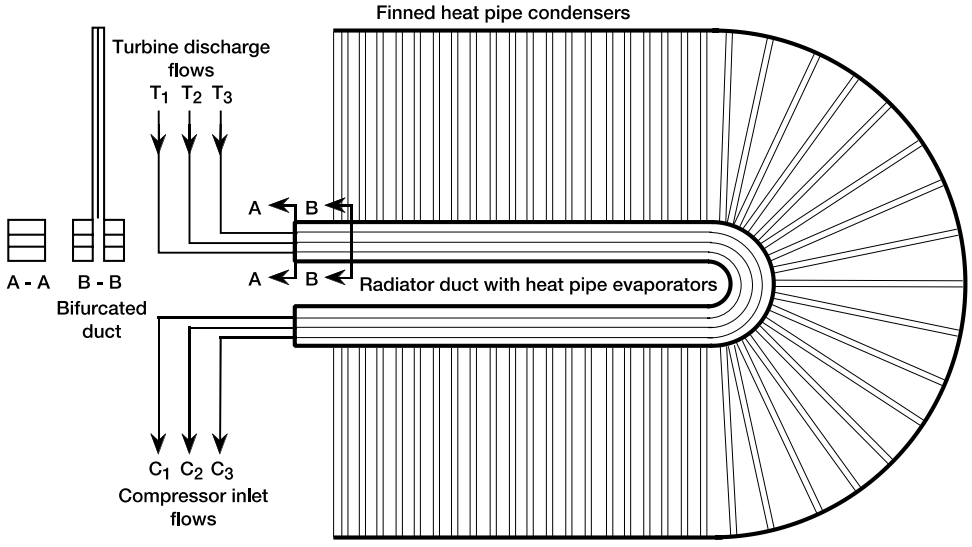

Figure 4. Flat segmented heat pipe radiator for a nuclear triple loop gas turbine power system. (Jushaz, 2002)

2.1.4 Portable Systems

Radiator systems follow the same basic principal for both portable units and stationary units. Portable units are those that attach to a moving unit such as Mars Pathfinder and Rovers. These units are not required to remove as much waste heat as their stationary counterpart due to the nature of the heat removal load, usually computers and smaller motors.

The first program to be launched was the Mars Pathfinder mission. The prime objective of the radiator was to transfer heat from lander and cruise electronics box during cruise, between 90 and 180 watts. The pathfinder radiator used active heat rejection system (HRS) with a mechanically pumped cooling loop. This was the first time active cooling system used in deep space. The working fluid for this system was Refrigerant 11 (CFC-11). The radiator assembly was located on the base petal of lander. The radiator design required that the system maintain single phase working fluid at temperatures between -100°C and 70°C with vapor pressure less than 100 psia, weigh less than 18 kg with cooling fluid, and have maximum power consumption less than 10 W. Tests of this system ran for 14000 hours, between Dec 1996 and July 1997, with no problems. Life test showed no major problems, projected pumped loop operation for many more years.

Following the success of the pathfinder mission the Mars Rover mission was started. This mission was to follow the pathfinder mission in exploring the surface of Mars. The rover was a redesign of the pathfinder radiator system to reduce weight. Its design consisted of two redundant pumps to circulate CFC-1, an accumulator for change in fluid volume, plumbing to circulate coolant, an integrated pump assembly capable of rejecting 90 to 180

watts at a temperature range of -80°C to 20°C, and a ten panel radiator on cruise stage. One of the major differences in design was the vent redesign. This redesign oriented the vent in downward perpendicular to the craft and increased nozzle diameter to shorten venting time. The end of the vent nozzle was changed from a flat surface to tapered end nozzle as well. Finally the vent heater was removed due to the decreased venting time needed. Other major changes included reducing number of panels from 12 to 10, decreasing the outside diameter of the tubing from 9.53 mm to 7.94 mm, and changing the paint from NS43G to Hincom made by Aptek.

2.2 Materials

2.2.1 Materials of Construction

The structural portion of the radiator system is an integral portion of the radiator design. The selection of this material has constraints similar to those of the actual radiator system. Properties for lunar construction materials should include high strength, ductility, durability, stiffness, and tear and puncture resistance, together with low thermal expansion (Reuss et al, 2006). The weight of the material is also of utmost importance to reduce the overall system weight. There are many material choices that have been used before in both low and no gravity environments. These include stainless steel, aluminum, aluminum compounds, polymer matrix composite materials, and titanium. One study carried out by NASA compared several materials for rigid lunar systems. The results of these approximate weight estimates showed that aluminum-lithium (2195) provided a 14% reduction, titanium (551) a 24% reduction, and polymer matrix composite (IM7.5250-4 BMI) a 26% reduction as compared to the baseline aluminum (2024-T3) design (Belvin et al, 2006). These weight estimations combined with cost and availability can be used to determine the

best material selection for the radiator structure.

2.2.2 Materials of Fin and Heat Pipe

Materials of construction for a radiator system can be anything that is reasonable for use in space systems. However, these materials must be able to withstand radiation and abrasive corrosion while effectively transferring heat to the environment. Other considerations include the operating temperature, working fluid interaction, and the emissivity of the material. Several materials have been considered for various designs. These include: titanium, copper, aluminum, and carbon composite. An overview of heat pipe properties is provided in Table 1. Currently aluminum is the most common material of construction used by spacecraft.

Copper has been used in radiator systems due to its good thermal conductivity (400 W/m·K at 398 K) and relatively low cost. While efficient at transferring heat the material itself has inherent flaws. The biggest drawback is the weight of a copper system. The density of copper is 8930 kg/m^3 making it the heaviest material of construction. Copper has a maximum tensile strength of 220 MPa, which makes it unable to withstand the majority of micrometeoroid strikes. Entire systems made using copper would be prohibitively expensive to implement in a space environment.

For extreme operating temperatures titanium is often used. It has poor thermal conductivity properties (20.4 W/m·K at 400 K) when compared to copper. Titanium does not react with most of the working fluids that react with other materials of construction. For systems requiring extremely high operating temperatures, titanium is also a viable option as its melting point is well above most system requirements at 1941 K. Unlike

copper titanium has a high maximum tensile strength of 900 MPa making it more able to withstand micrometeoroid strikes. The density of titanium is 4506 kg/m^3 thus lighter than copper but heavier than other options. The biggest drawbacks to titanium are the cost to fabricate the parts as well as its low thermal conductivity. For these reasons titanium has been relegated to specialized systems.

The most prevalent material used in heat pipe systems for space is aluminum. Aluminum has the thermal conductivity (255 W/m·K at 398 K) less than that of copper but greater than titanium. It also has a higher maximum tensile strength, 483 MPa, while having a low density, 2800 kg/m^3. This makes it an ideal candidate for space applications as it can withstand a majority of micrometeoroid strikes while minimizing the weight of the entire system.

A fairly new material for radiator fabrication is a carbon composite material. Weaving carbon fibers together in either an omni-directional or multidirectional weave makes carbon composite material. The principles of the manufacturing process used in laboratories are well documented, but the technology used in production is normally regarded as confidential (Windhorst and Blount, 1997). This material is lightweight and durable while have acceptable heat transfer capabilities. The thermal conductivity for carbon composite material is 202 W/m·K at 393 K with a density 1780 kg/m^3. The maximum tensile strength for carbon fibers is 5650 MPa. The carbon has a similar thermal conductivity to aluminum while being about 40% lighter and 93% stronger. Composite materials due have significantly higher effective emissivities than bare metallic liner materials. (Klein et al, 1993) A carbon composite radiator was a success and proved that the technology can work to reduce spacecraft weight (Teti, 2002). The major consideration

for this technology is the cost and fabrication time (Vaughn, et al, 1998). The benefits of the carbon composite material make it a worthwhile candidate for a space radiator system.

Table 1. Overview of heat pipe material properties.

Material	Thermal Conductivity (W/m·K)	Density (kg/m^3)	Tensile Strength (MPa)	Emissivity
Copper	400 (@398 K)	8930	220	0.75
Titanium	20.4(@400 K)	4506	900	0.9
Aluminum	255 (@398 K)	2800	483	0.3
Carbon Composites	202 (@393 K)	1780	5650	1.0

2.3 Heat Pipe

Heat pipes have been successfully used for the last fifty years in space with few issues. Since a heat pipes design contains no mechanical moving parts and typically require no maintenance. Heat pipes have been proven to handle multiple freeze-thaw cycles (Elliott, et. al., 2003). A benefit of the heat pipe system is to use parallel heat pipes throughout the radiative surface. This prevents any micrometeoroid strikes from disabling the radiator system completely (Juhasz, 2001). Though the general design has not changed much over time the materials of construction have changed to produce a lighter weight and more efficient system. This coupled with the advances in optimization software allow for this field-tested design to still be relevant in the current consideration for designs.

There are a couple of drawbacks to the heat pipe design. The largest constraints are the weight and area required to transport this type of system. Since the radiator will be payload on a shuttle or rocket, the area required to move it along with its weight are major considerations. A radiator system can be as much 40% of the overall mass an entire system

(Tagliafico and Fossa, 1997). The other drawback is the efficiency of the heat pipe itself. Lunar and space environments provide no means convective heat transfer. This means that the heat pipe must be able to radiate enough heat to meet system requirements.

Heat pipes are a tried and true system for heat transfer in a purely radiative environment. They have been successfully used numerous times in low and no gravity environments. This type of design allows for a space radiator to be composed of a multiplicity of independently operating segments, a random micrometeoroid puncture of the radiator would result in the loss of only the punctured segment, not the entire radiator (Juhasz, 2001). Combining this time tested design with modern materials of construction and current design optimization techniques will provide a feasible radiator design that does not require years of research and study to be operational. The heat pipe design utilizing a lightweight ceramic woven fabric for structural strength along with a metallic liner for working fluid retention can yield significant reductions in the mass of radiator systems (Antoniak et al., 1991). Initially intended for high temperature systems, the technology can be extended to cover a broad range of temperatures by properly selecting alternate heat pipe working fluids and compatible liner material (Juhasz, 1998).

2.4 Fin and Fin Integrated with Heat Pipe

Fins are used in radiator systems to increase the surface area over which heat is transferred. Through the use of fins the surface area is increased while adding a minimal amount of weight to the system. This allows for the radiator system to be smaller and lighter while having the same overall surface area of a larger system that has no fins. In space applications, the fins allow for a larger surface to radiate heat into space. The heat radiated by the fins is shown to be proportional to the cube of the heat pipe temperature, two-thirds

power of the emissivity, and one-third power of the thermal conductivity to density of fin material (Naumann, 2004). Once the heat transfer is known the dimensions of the fins can be calculated. The optimum dimension for the fins depends on the opening angle and the emissivity and the profile not the specific values of fin heat dissipation or the fin volume (Krikkis & Razelos, 2002). The effectiveness of the fins also needs to be calculated to determine whether fins are necessary to the system. Effectiveness of the fin expressed through apparent emittance, the ratio of actual total radiative heat loss to the ideal heat loss by a black, isothermal fin (Krishnaprakas & Narayana). If the effectiveness is calculated to be less than two the fins are not necessary to the system (Incropera and DeWitt, 1996).

There are two primary types of fins for radiator systems; solid fins and heat pipe fins. Fins that attach directly to the heat source are considered solid fins. Heat pipe fins are part of the heat pipe system and remove heat from the system to working fluid and radiate the heat into space through the fins attached to heat pipes. These fins can either be flush mounted or inserted into the heat pipe (Bowmann, Moss, et al., 1999). Then there is the geometry of the fin. The fin shapes that are most common are rectangular, trapezoidal, and triangular.

The purpose of adding fins to a system is to reduce weight while maintaining heat transfer area. For this reason, heat pipe fins are beneficial when weight is a design parameter (Bowmann, Storey, et al, 1999). Heat pipe fins typically weigh less than the corresponding solid fins given by a required heat transfer area. This is due to the heat pipe being hollow. Because of the proximity of the working fluid to the heat transfer area, heat pipe fins are usually more efficient than solid fins for radiative environments (Bowmann and Maynes, 2001).

Fin geometry is the other major area of concern in design. Rectangular fins provide the greatest area for heat transfer. However, these fins also increase the weight of the radiator significantly. Trapezoidal fins allow for a slight reduction in weight but without a significant reduction heat transfer area. Triangular fins are half the weight of their rectangular counterparts and transfer between five and fifteen percent less heat (Schnurr, 1975).

2.5 Radiator Fluid Selection

Almost any fluid can be used in a radiator system. The type of fluid is based on the materials and temperatures of the system. The most common working fluids are water, ammonia, and exotic materials such as liquid metals. Other materials are suitable on a case-by-case basis.

Ammonia is the most common fluid used in extraterrestrial radiator applications. This is due to its low freezing point and vapor temperature. For operating temperatures between 200 and 300 K ammonia is an ideal working fluid (Juhasz, 2007). Ammonia, in anhydrous form, is compatible with many typical materials of construction including aluminum, nickel, ceramic and stainless steel. It does corrode materials such as titanium and copper and other materials of construction should be considered.

For slightly higher temperatures, purified water is an option. Water is useful when the radiator operating temperature is between 300 and 500 K (Juhasz, 2007). This prevents the water from freezing or remaining in a vapor state. However, if freezing is of concern during times of shutdown, additives such as propylene glycol can be added to the water to lower

the freezing point. Purified water is also compatible with most common types of structural materials use in radiator fabrication.

When dealing with extreme temperatures, such as those for nuclear power plants, the radiator working fluid is typically a metal or material that similar characteristics of a metal. These are typically used in temperatures of 700 K and greater (Keddy, 1994). For this reason, liquid metals are necessary for the operation of the radiator system. Liquid metals are extremely corrosive. The corrosion rate is sensitive to the operating temperature and the temperature change in the system (Thompson, 1961). The specific working fluid will dictate the materials compatibility with the radiator structural material. If the two are incompatible a liner in the radiator can be used to prevent contact as is done in Jushaz's radiator design.

2.6 Wick Design

Radiator wicks are used to transport the condensed liquid from the cold region of the heat pipe to the hot region in low and no gravity environments. There are various wick designs and materials. Three primary designs are: slab wicks, arterial wicks, and groove wicks. Each design provides benefits for various radiator systems. The other wick consideration is the material of which the wick is made.

The most basic design is the slab wick. In this design most of heat pipe filled with highly permeable screen or other material. The vapor then condenses on the wick down the pipe to be transported back to the evaporator section. This design is simple and easily constructed. The major drawback is that there is a significant increase in weight.

Arterial wicks utilize a mesh or screen that covers the inside of the heat pipe. As the fluid condenses on the walls of the heat pipe, the wick moves the fluid back to the evaporator section. This design is efficient in that as the heat transfer through condensation is taking place the fluid is already in the wick ready to be transported. This allows for a thin layer of wicking material. An arterial design works well with alkali metals as well as most other general operating fluids. The only drawback is that it is difficult to keep the wick primed when using water at higher temperatures.

Grooved wicks provide a simple design by simply machining grooves into the heat pipe material. The fluid condenses in the groves where it is transported back to the evaporator section through the channels. These types of wicks offer easily reproducible behavior while not adding additional weight to the system. However, this wick design is only feasible for piping materials that can reasonably be machined.

The most common wick material in space radiator systems with water as a cooling fluid is copper. Copper can be used in systems operating at less than 425 K due to its low melting point. For systems operating over 425 K titanium is often considered for the wick material.

2.7 Radiator Design Optimization

The radiator design optimization uses three major factors in optimization: heat transfer rate, surface area of the radiator, and mass of the radiator. Fin design is an additional optimization constraint when it applies to the design. Optimization can be done several ways. The two primary approaches are optimizing mathematical models or using computer programs to optimize a specific design. Each method has its strengths and weaknesses.

Mathematical models use fundamental equations to optimize portions of the radiator. The general goal of radiator optimization is minimize the radiator mass for a given heat storage and dissipation (Roy and Avanic, 2006). Using equations a general solution for optimum design can be achieved. The types of optimizations can be linear, optimizing the ratio of fin mass to heat pipe mass (Naumann, 2004), or using special decomposition techniques to determine the maximum heat transfer rate per unit mass (Arslanturk, 2006). This type of optimization provides a general form of optimization that can be altered to optimize similar designs. The major drawback to this form of optimization is that it is often times limited to a specific design. This is due to assumptions and addition/removal of terms from the overarching equations.

Computer simulation modeling also allows for optimization of radiator design. Programs like FLUENT®, Thermal Desktop®, and Space Nuclear Auxiliary Power Analysis System (SNAPS)® optimize a specific design that has been drawn. The different programs have different approaches to obtaining an optimized design. SNAPS® uses a flowsheet design often used in chemical processing. Flowsheet software is useful for performing steady-state heat and mass balances, sizing equipment, and running cost analysis. (Diwekar and Morel, 1993) FLUENT® is a useful commercial software tool in the design of a single small scale system, such as a single heat pipe and fin assembly while Thermal Desktop® is ideal for large scale design of an overall system and the surroundings (Siamidis, 2006). These modeling programs can produce numerical results of theoretical operating parameters. This allows the designer to overlay the different design parameters to optimize the system around desired operating parameters. The downside to this is every

design done using a computer program needs to be modeled and optimized to determine the optimum design.

Chapter 3

Theory and Numerical Methods

There are many aspects of design that are considered in heat pipe design. The governing equations of continuity, momentum and energy prevail in the system. Heat transfer equations are then used to determine the amount of energy that can be transferred to the surroundings. Computational fluid dynamics (CFD) programs use the above equations along with the proper boundary conditions and additional input parameters, based on the needs of the individual design, to numerically model a system.

3.1 Governing Equations

The energy equation is of utmost importance in radiator system design. This equation describes the energy transfer both inside the system and energy transmission to the surroundings. This transfer for the fluid is described by Equation 1.

$$\frac{\delta}{\delta t}(\rho \cdot E) + \nabla\big(v(\rho \cdot E + p)\big) = \nabla \cdot \big(k_{eff} \cdot \nabla T - \sum_j \ h_j \cdot \vec{j}_j + \big(\bar{\bar{\tau}}_{eff} \cdot \vec{v}\big)\big) + S_h$$

(1)

The effective conductivity is given as k_{eff} (W/m·K). This effective conductivity is the combined ability for all materials of a specific region in the design to conduct heat. The diffusion flux of each possible component is represented by $\vec{J_j}$(kJ/m^2·K). This flux accounts for the rate at which an individual component diffuses. This flux term is a summation of the sensible enthalpy, h, multiplied by the diffusion flux for every component being considered. Energy is represented by E (kJ) in the above equation. However, the energy is a function sensible enthalpy, pressure, density, and kinetic energy as shown in Equation 2.

$$E = h - \frac{p}{\rho} + \frac{v^2}{2} \quad (2)$$

The sensible enthalpy used in energy equation above for an incompressible fluid is shown in Equation 3.

$$h = \sum_j \ Y_j \cdot h_j + \frac{p}{\rho} \quad (3)$$

For the portion of the heat pipe that is in vapor form, the energy is represented by an ideal gas as represented in Equation 4.

$$h = \sum_j \ Y_j \cdot h_j \quad (4)$$

The Y_j term is the mass fraction the component that is in the gas form and the h_j term is the sensible energy for the component. Equation 5 shows how the sensible enthalpy for each component is calculated where T_{ref} is 298.15 K. The specific heat for a component is defined as $c_{p,j.}$

$$h_j = \int_{T_{ref}}^{T} c_{p,j} \cdot dT \quad (5)$$

The momentum equation is used in heat pipe design to describe the fluid movement in the heat pipe. Since the fluid in the heat pipe can be in one or two phases this equation it must account for both the liquid and vapor phases of the working fluid. FLUENT® also couples the momentum equation with the mass conservation equation. The conservation of

mass is calculated using Equation 6, which shows that mass is a function of density, velocity, and pressure change with respect to time.

$$\frac{\delta \rho}{\delta t} + \nabla \cdot (\rho \vec{v}) = S_m \tag{6}$$

The momentum equation is also a function of velocity, density, and pressure change. This equation, Equation 7, also takes into account stress tensors as well as gravitational and external body forces.

$$\frac{\delta}{\delta t}(\rho \vec{v}) + \nabla \cdot (\rho \vec{v} \vec{v}) = -\nabla p + \nabla \cdot (\bar{\bar{\tau}}) + \rho \vec{g} + \vec{F} \tag{7}$$

3.2 Fundamentals of Radiation Heat Transfer and Heat Pipe Efficiency

There are three types of heat transfer that should be considered for radiator design. These heat transfer models are convection, conduction, and radiation. All of these methods depend primarily on temperature gradients to move the heat. The difference is a transfer constant parameter unique to each equation.

Convection is a method of heat transfer by which heat is transferred due to bulk fluid movement. All environments that include a fluid have convection as a major component of heat transfer either to or from the surrounding fluid. Since fluid motion is a function of temperature fluctuations, there are few places that convection does not occur. In Equation 8 it is shown that convection is a function of the heat transfer coefficient (h_c), the surface area of heat transfer (A), and the temperature difference.

$$Q = h_c A dT \tag{8}$$

Conduction heat transfer considers the heat transfer through a solid or fluid due to contact. Equation 9 shows that conduction is a function of the thermal conductivity of the material (k), the surface area of heat transfer (A), and the temperature gradient. This form of heat transfer is a primary concern when there are large distances, thicknesses, which are under consideration or in the case of heat transfer though a substance is the primary concern.

$$Q = kA\frac{dT}{dx} \tag{9}$$

The final form of heat transfer is radiation. For most situations radiation is negligible as compared to convection or conduction transfer. However, for extraterrestrial environments it is the primary form of heat transfer to or from a system. Due to the lack of atmospheric ambient fluid movement convection heat transfer is not a feasible design consideration. For this design the walls of the heat pipe are relatively thin and made of a highly conductive material thus making conduction a negligible design consideration. Since this system would operate on the lunar surface, radiation heat transfer is the primary source of heat transfer.

The materials of construction can be classified as either blackbody or grey body. The blackbody radiator, also called the ideal radiator, absorbs all the energy it encounters reflecting nothing back into the surroundings. It provides a theoretical maximum value for a design. Typically blackbody radiators are considered theoretical only due to the perfect transmission of energy. The energy transfer in an ideal system is due only to the Stefan-Boltzman constant, surface area, and operating temperature raised to the fourth power as shown in Equation 10.

$$Q_{ideal} = \sigma A T^4 \tag{10}$$

The other type of radiator is a grey body radiator. This type of radiator both absorbs and emits energy into the system. The equation for grey bodies is similar to that of blackbodies. The grey body equation contains the effect of the material, emissivity, which accounts for the imperfect radiation. The basic equation for radiation heat transfer is shown in Equation 11 and adds the effect of emissivity and the sink or surrounding temperature raised to the fourth power.

$$Q_{real} = \sigma \varepsilon A_{rad}(T_{in}^4 - T_{sink}^4) \tag{11}$$

This equation considers the emissivity, ε, the Stefan-Boltzman constant, σ, and the temperature of the surface and surroundings. The emissivity of an object is the objects ability to radiate heat from the surface. For an object that can radiate all the heat from its surface the emissivity is one. This type of object is a black body and is generally considered theoretical. Most substances cannot disperse all the heat they contain via radiation from their surface. These are considered grey body radiators. They have an emissivity ranging from zero to one. The emissivity for a substance is determined by empirical means and is considered a property of that material. By including the emissivity the amount of heat transferred from the surface is decreased from that if its black body counterpart; however, this provides a more accurate depiction of the actual expected heat loss. The Stefan-Boltzman constant is a proportionality constant that is based on the Stefan-Boltzmann Law. This law is the governing law for black bodies that states the radiation heat emitted from a substance's surface is proportional to the absolute temperature to the fourth power.

To determine the efficiency of the heat pipe design the theoretical maximum is compared to the actual value as given in Equation 12. For theoretical calculations this would be the comparison of the black body radiation power to that of the grey body. For the computer aided design the efficiency would be the comparison of the computer design power to the theoretical grey body value. Hence, the following equation would hold.

$$\eta = \frac{Q_{calculated}}{Q_{theoretical}} \tag{12}$$

In an ideal situation the power calculated would be nearly the power that theoretically would be dispersed.

3.3 Models Used in FLUENT

FLUENT® is a commercial CFD software which can be readily used in radiation heat transfer modeling. The program uses various numerical methods to determine temperature and power results. There are five numerical solving techniques that are included in FLUENT®. These solvers are discrete transfer radiation model (DTRM), P-1 radiation model. Rosseland radiation model, surface-to-surface (S2S) radiation model, and discrete ordinates (DO) model. Each method of solving has its valid uses and limitations. These are briefly described below.

Advantages and Limitations of the DTRM

DTRM is a relatively simple model that applies to a wide range of optical thicknesses. Increasing the number of rays in the calculation can increase this models accuracy. However, there are certain limitations for this model. The model assumes that all surfaces are diffuse and exhibit grey body radiation. The effect of scattering is not considered in the

DTRM model. It is not able to handle parallel processing or sliding meshes and can be time consuming for a large number of rays.

Advantages and Limitations of the P-1 Model

The P-1 model uses the radiative transfer equation (RTE) to make the design easy to solve. The RTE states the a beam of light loses energy through the divergence, absorption, and scattering and gains energy from light sources in the medium and scattering of other beams towards the beam of light. This model also takes into account the effect of scattering. For optically large thicknesses and complex geometries the model is also acceptable. There are certain limitations for this model. The model assumes that all surfaces are diffuse and exhibit grey body radiation. When used to solve more complex geometries accuracy is lost. It is not able to handle parallel processing or sliding meshes and can be time consuming for a large number of rays. The P-1 model may over-predict radiative fluxes when localized heat sources or sinks are present.

Advantages and Limitations of the Rosseland Model

The Rosseland model does not solve for incident radiation like the P-1 model. In not doing this step the model has a faster computational time and does not require the same amount of memory. However, there are a couple of limitations for this model. The Rosseland model can only be used for extremely optically thick materials. Also, it cannot be used in conjunction with a density based solver thus requires the pressure based solver to be enabled.

Advantages and Limitations of the S2S Model

The surface-to-surface (S2S) radiation model used in modeling enclosed radiative transfer systems. The S2S model has a faster solving time than other models though depending on geometry. This is particularly true for polyhedral cells. This model is often used when modeling systems for extraterrestrial heat rejection systems.

The limitations of the surface-to-surface model are that it assumes all surfaces grey surfaces that are diffuse. This model cannot be used for participating radiation designs, non-conformal interfaces, or symmetry or periodic boundary conditions. Also of note is that memory requirements increase rapidly if view factors are not clustered.

Advantages and Limitations of the DO Model

The discrete ordinates model has benefits in that it can be used over a vast range of optical thicknesses. It can be used to solve problems that are encompassed in other models. This model can also be used to evaluate semi-transparent walls. The time and memory for calculations is modest compared to other models.

Chapter 4

Benchmark and Validation Studies

An independent mesh study was conducted on a basic design of a heat pipe with integrated fin. This was done to ensure that the resulting values of the program were independent of the mesh size. In doing a mesh independent study, the results of the model represent a true and accurate value. Once the minimum mesh size required for the design was determined the wick study and benchmark could be calculated.

Next a wick study was conducted. For this design the wick was not modeled. Since the wick is used to transport the fluid in the heat pipe the wick effect had to be considered. To determine a numerical representation of the equivalent wick performance, two papers Woloshun, et al. (1993) and Dickenson (1996) that evaluated the temperature profile of the wick were evaluated. The results of this were used to simulate the effect of the wick in the design.

Benchmarking is done to ensure that the user and the program are producing valid results. For this purpose two separate designs were used as benchmarks. One benchmark was to validate FLUENT® and the other to validate user results. The benchmark design is that of a heat pipe design that closely relates to the design being considered. This benchmark allows for the comparison between computer design and laboratory and actual working data. This can show any biases in the design and potential problems in the set-up conditions.

4.1 Validation Study

4.1.1 Purpose

The mesh independent study is used to determine the point in meshing a design that the results vary only slightly with a change in the mesh. This value can then be used to assure that the number of nodes or cells used exceed this minimum value. If the minimum value is exceeded, the results are no longer dependent on the size of the mesh. Performing a mesh independent study assures that the design is only changing with boundary conditions and not with mesh conditions.

4.1.2 Methodology

The most general design of a heat pipe with integrated fin was selected for this study as shown in Figure 5. This design consisted of a heat pipe with integrated fin. The heat pipe had an outer diameter of 25 mm and an inner pipe diameter of 23 mm. The design had a fin length of 25 mm and had a thickness of 2 mm. The heat pipe and fins were 300 mm. The end caps were also 2 mm thick. This selection was due to the fact that this design was the starting point for all other models. The mesh size was varied from 4738 cells to 19609 elements. The temperature along the pipe at various intervals was analyzed as a function of the number of cells. This was then evaluated to determine the minimum number of cells necessary for the mesh to no longer affect the temperature results.

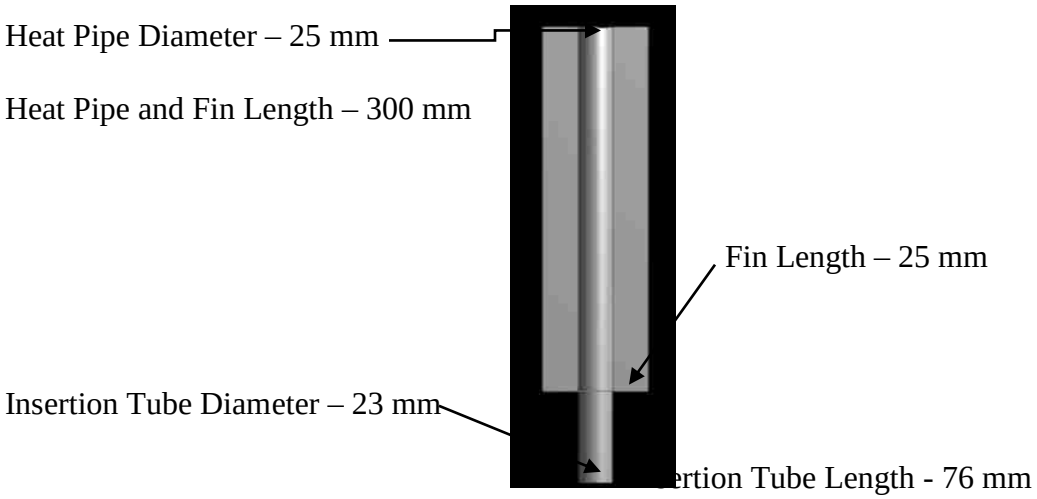

Figure 5. Three-dimensional design for validation study.

Four mesh discretizations were analyzed. The analysis included 4738, 9486, 11461, and 19609 number of elements. The first represented a coarse mesh while the final represented a fine mesh with high smoothing. The values in between are values that were easily represented to analyze the transition section to determine the minimum mesh size for independence.

4.1.3 Results

The validation study was carried out on the heat pipe with integrated fin. This showed that the temperature gradient was somewhat dependent on the mesh when the number of cells was less than 11461. However once the number of elements exceeded 11461 the temperature became stable. The following, Figure 6, shows the graphical representation of the above results of temperatures every 75 mm along the outside of the heat pipe.

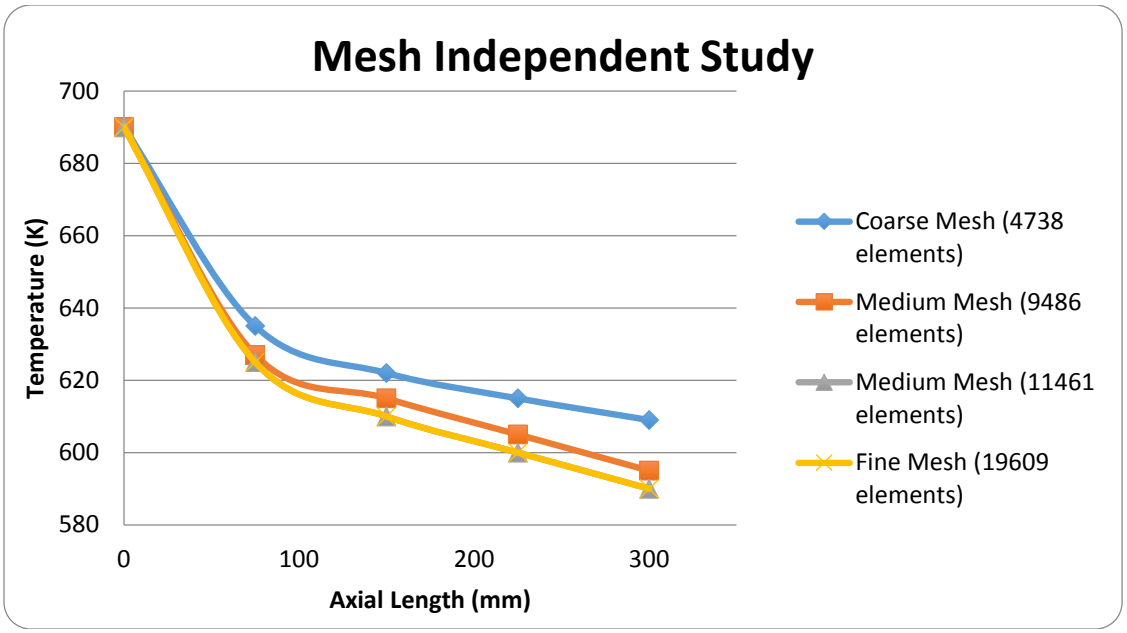

Figure 6. Results of independent mesh study.

As this is a simple geometry, the relatively small number of cells necessary for the temperature to become independent of the mesh is expected. By using a mesh in the 12000 range the mesh independence of the various geometries and fin comparison can be expected.

4.2 Wick Performance Simulation

In order to accurately describe the performance of the heat pipe the performance of the wick characteristics had to be determined since the wick structure was not to be modeled in this design. Several papers, Woloshun, et al. (1993) and Dickenson (1996) describing the performance of the wick were studied. From the results of these papers a profile was created.

The papers of Woloshun, et al. (1993) and Dickenson (1996) were evaluated to determine the behavior of heat pipe slab wick. These papers showed similar profiles regardless of the operating temperatures or the ambient temperatures. Since there seemed to be no dependency on these conditions it was assumed that this general profile was standard among all heat pipes in low and no gravity environments. The thermocouple results of these papers were taken and entered into Excel to generate two graphs. From this graph a linear regression was done using Excel, and a third degree polynomial equation, Equation 11, was generated. In this equation temperature, T, is given as a function of axial length, x.

$$T = -1.4x^3 + 1.4893x^2 - 0.6724x + 0.9139 \quad (13)$$

Though there were actually two equations generated, the equation with the lower variance was selected to model the pipe interior. This equation was then used to create a user-defined function (UDF) profile in FLUENT® to account for the equivalent wick performance in the heat pipe. This technique is adequate for this design in that the interior geometry is unchanged among all the heat pipe designs. However, this equation only represents a slab wick design and cannot be used to represent any other wick configurations.

4.3 Benchmark Study

4.3.1 Heat Pipe Design

This goal of this research was to investigate and compare the operation of a microgravity, liquid-metal heat pipe in both laboratory and operational settings. There was a project supported by the United States Air Force Institute of Technology as part of a

Master's Thesis. (Dickenson, 1996) Heat pipe start-up from a frozen state, start-up from a pre-heated state, steady state operations, as well as various wick designs for the afore mentioned were considered. The research conducted on the heat pipe containing the annular wick was of interest as it closely mimicked the Juhasz's design to be modeled.

4.3.2 Dimensions of Heat Pipe

The design of the heat pipe tested by Dickenson (1996) also closely resembled that of the Juhasz's design. The heat pipe tested was 610 mm in length, with 521 mm being the condenser and 89 mm being the evaporator. The heat pipe outer diameter was 23 mm in diameter and had a wall thickness of 0.89 mm. Stainless steel 304 was used to make the heat pipe and the wick material. The working fluid to convey the heat transfer was potassium.

4.3.3 Boundary Conditions and Operating Parameters

This design had several operating temperatures. For the sake of comparison the 700 K operating temperature was the trial that was used for comparison. The laboratory tests were carried out in what is characterized as "room temperature" without a value provided. The shuttle flight test data had rejection temperatures ranging between 10°C and 35°C. The wick boundary condition was set using the wick study values to approximate the performance of the wick.

In this trail the parameters for the materials were provided. A thermal conductivity of 21.2 W/m·K was given for the 304 stainless steel pipe material while the wick material had a thermal conductivity of 29.11 W/m·K. The heat capacity for 304 stainless steel was 569.5 J/kg·K. Finally, the density for the stainless steel was given to be 7900 kg/m^3.

4.3.4 Numerical Modeling of Heat Pipe Design

A numerical modeling of heat pipe design using FLUENT® was created using the given parameters for the laboratory and shuttle data. The design included a 610 mm long heat pipe with an integrated fin. The condenser section of heat pipe was 521 mm in length with an outer diameter of 23 mm. The evaporator section was 89 mm in length and had an outer diameter of 22 mm. The schematic of this is shown in Figure 7. The heat pipe had a wall thickness of 2 mm. Stainless steel 304 was used to in the modeling of the heat pipe. The working fluid to convey the heat transfer in the model was potassium.

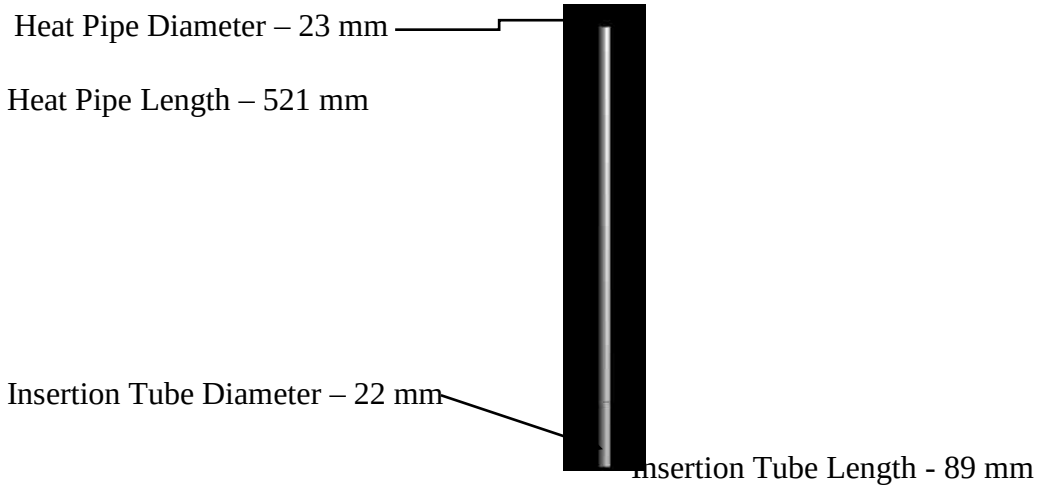

Figure 7. Schematic of heat pipe with integrated fin from numerical modeling design for benchmark study.

4.3.5 Comparison of Numerical Results

This numerical data obtained from FLUENT® was compared to the results provided by Dickenson (1996). The numerical results provided the same temperature profile as the laboratory and flight tests data gave as shown in Figure 8. Both the numerical results

obtained from FLUENT® and the flight test data begin at 600 K, drop to the 480 K range along the condenser section, and drop quickly at the end cap to about 300 K. The numerical values obtained from FLUENT® were slightly higher than that of the benchmark study as shown in Table 2. However, the values were close enough to believe that FLUENT has accurately provided the satisfied numerical results compared to modeled results obtained from the laboratory data.

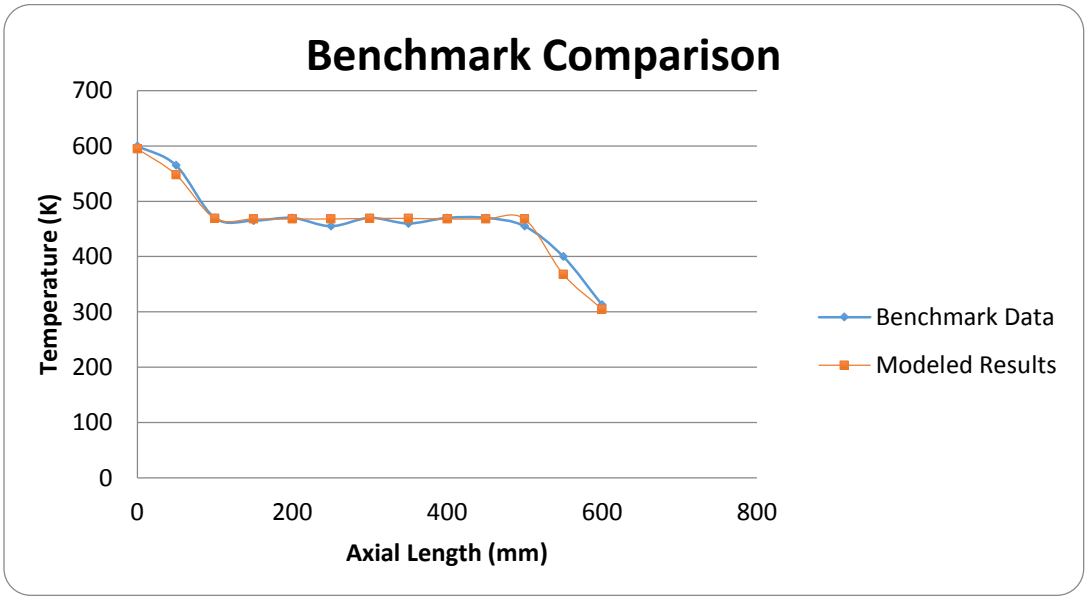

Figure 8. Axial length versus surface temperature comparison for benchmark and numerical results.

Table 2. Benchmark and FLUENT data comparison

Axial Length	Benchmark	FLUENT	
	Results	Modeled Results	Percentage Difference
mm	K	K	%
0	600	595	0.83
50	565	548	3.01
100	470	469	0.21
150	465	468	0.64
200	470	468	0.43
250	455	468	2.78
300	470	469	0.21
350	460	469	1.92
400	470	468	0.43
450	470	468	0.43
500	455	468	2.78
550	400	386	3.50
600	313	305	2.56

The numerical modeling of heat pipe design provides a smoother temperature profile in the condenser section of the heat pipe. It does not exactly mimic the behavior of the test data in the first and last 100 mm of the pipe. The difference in the FLUENT and benchmark data is a result of smoothing within FLUENT; however the differences in temperature are less than 3.5%. Because FLUENT shows a greater decrease in the temperature of the heat pipe in the first and last 100 mm, the computer model is likely under reporting the power output of the heat pipe.

Chapter 5

Results and Discussions

Due to the size constraints of a shuttle load the radiator would need to be designed in segments. The reason for this is twofold. This design will make for easier transport than one large system and in minimizes the risk of complete failure if the operational radiator is damaged. For this design an individual heat pipe is to be modeled using FLUENT®.

The individual heat pipe design is based on that of Albert Juhasz (1998). In his publication "Design Considerations for Lightweight Space Radiators" he provides a design consisting of a heat pipe 25 mm in diameter, 300 mm in length, with a 1 mm thick wall. The design also specifies fin dimensions of 25 mm in width and 1 mm thickness running the entire length of the heat pipe.

Every design contained an insertion portion that would be used as the evaporator section. This portion would be inserted in a main pipe that carried a high temperature fluid. The length of the evaporator section was 76 mm and had an outer diameter of 24 mm. This section also had a wall thickness of 2 mm due to constraints of the program and the mesh. The specifications for this design are shown in Figure 9.

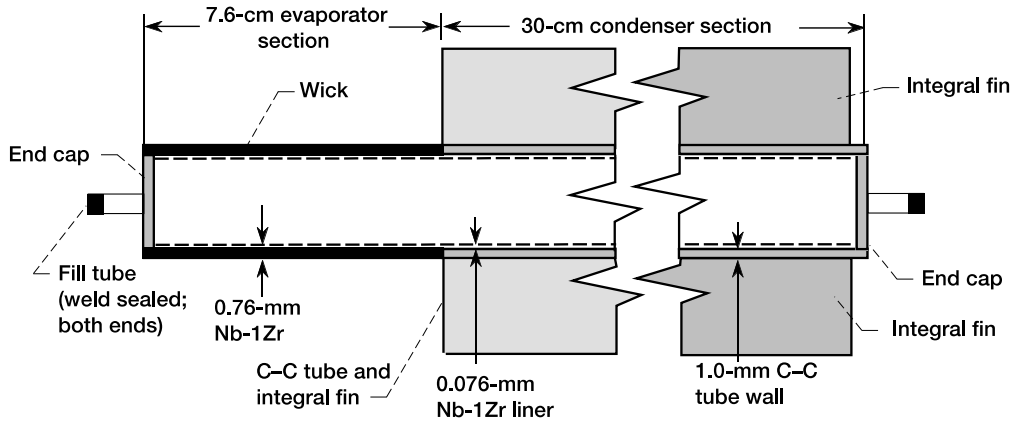

Figure 9. Heat pipe design. (Juhasz, 1998)

The initial goal was to determine that the heat pipe design was the best design for this radiator design. This was done by comparing various geometries. Rectangular solid, cylindrical solid, cylindrical solid with fins, heat pipe without fins, and the above design were modeled and the results compared. All the designs maintained the same radiation surface area and had the same parameters used for evaluation.

Once the heat pipe design was proven to be a feasible design, the fin length needed to be evaluated to determine the best length in order to minimize the size while maximizing the heat transfer. This was accomplished through varying the ratio of fin width to fin length. The ratio of fin length to width was evaluated at 0 (from the above design), 0.25, 0.5, 0.75, 1 (from the above design), 1.25, and 1.5.

The temperature profiles and power output of the designs outlined above were modeled using FLUENT®. The designs were created in FLUENT® and modeled using the P-1 radiation model. The P-1 model was used due to a relatively simple geometry but the need to account for scattering. Results obtained from FLUENT® are shown as positive, for incoming power values, or negative for power that is leaving the system. As is mentioned

in Chapter 3, the P-1 model tends to over predict the radiative fluxes. In those cases the net flux is given as a negative value. Due to this possibility of over prediction, a relative error was calculated for each design. This error calculation is used as a design control to maintain the discrepancies in the results to less than 5%. Along with the radiation area and volume of the various designs were determined using FLUENT® analysis. These values along with power and temperature data were used to compare geometrical shapes, pipe width to length ratios, and profile data.

5.1 General Methodology

The basic steps were used in each design. To begin FLUENT® was chosen in the ANSYS Workbench to create a new project. Then the geometry was created using the geometry module. The geometry varied based on the individual case and these designs are discussed in their relative sections. Once the geometry was created and saved, the mesh module was selected. In these section individual components of the design such as the insertion tube, fins, end cap, and pipe interior were named in order to be able to set individual boundary conditions or look at individual performance once the simulation was completed. After all the components were named, the mesh was generated and the file saved.

FLUENT® was selected from the workbench screen. Once the meshed model opened, the energy equation was enabled and radiation model was selected. A screen appeared to allow for the selection of a specific radiation model. From this screen, the P-1 model was selected. The scattering is assumed isotropic and the scattering coefficient remained zero. Materials properties were created for the carbon composite material. The fluid was set as potassium using the parameters form the benchmark study. Boundary conditions were set

for each of the defined areas of the geometry. The boundary conditions were standard for each design. The solid designs did not contain a pipe interior and the designs without fins did not have conditions set for them. The insertion tube was set at a constant temperature of 700 K. The outer wall and fins boundary condition was defined by the radiation parameters of emissivity of 0.8 and external temperature of 230 K. The pipe interior, as discussed above, was defined using a user-defined function to approximate the equivalent wick performance.

5.2 Parametric Comparison

The first objective was to consider various geometries for a heat pipe design. The geometries include a rectangular solid, a cylindrical solid, a cylindrical solid with fins, a heat pipe, and a heat pipe with 25 mm fins. This was done to ensure that a heat pipe was a feasible design choice in both power output and power per unit mass.

5.2.1 Rectangular Solid

The rectangular solid consisted of a base rectangle of 22 mm by 22 mm. This was extruded to a length of 600 mm. The schematic of this design is shown in Figure 10. This geometry had a power input of 153.59 W and an output of 157.00 W. The raw data from FLUENT® is shown in Table 3. This power output translated to a power per radiation area of 2963.94 W/m^2 and a power per mass of 165.68 W/kg. As compared to the theoretical value for the radiation area the efficiency of the rectangular design is 27.5%.

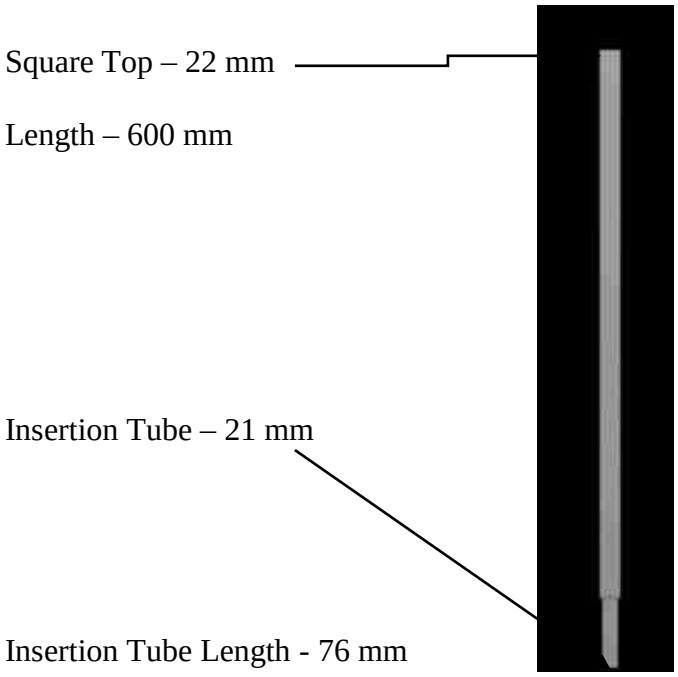

Figure 10. Schematic of rectangular solid.

Table 3. Power values for rectangular solid.

Rectangular Solid		**Power (W)**
Insertion Tube		153.59276
Outer Radiation Surface		-157.00218
Net		-3.4094201
Error	2.171575006	%

The temperature profile of the rectangular solid is shown in Figure 11. The profile is what would be expected of a solid material. Since the only means of heat transport through the solid is conduction, the temperature is much higher near the insertion tube and drops along the axis. The insertion tube temperature is held at 700 K and the end temperature is 410 K. The temperature drops 200 K in the first half of the rectangular solid. This can be compared to the 90 K drop along the second half.

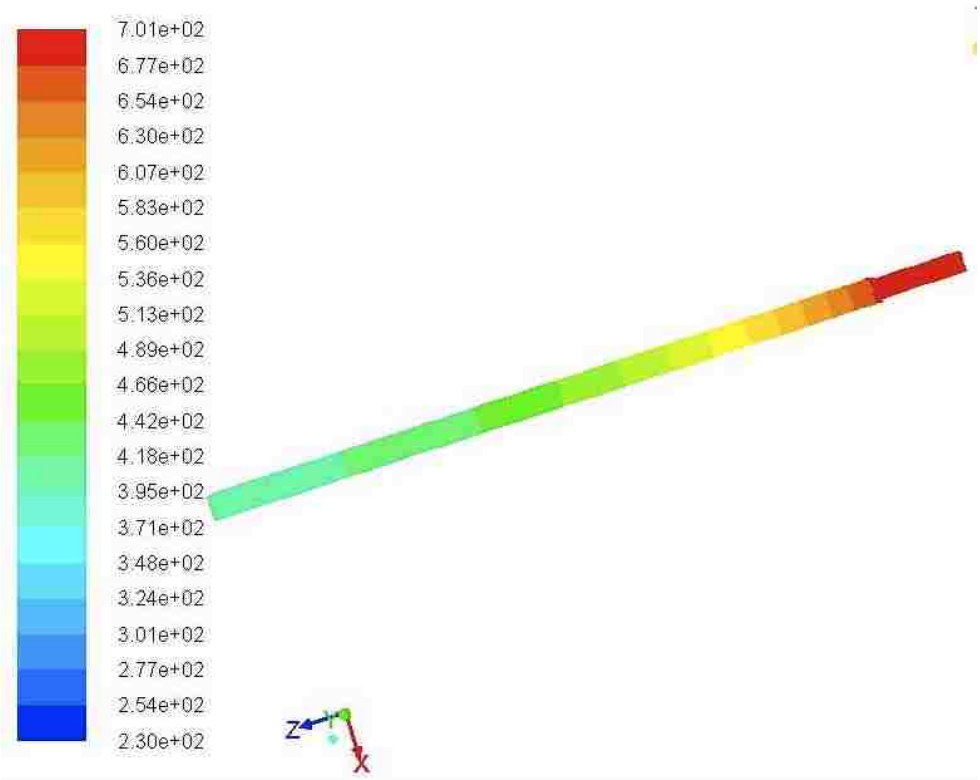

Figure 11. Temperature (K) profile of rectangular solid.

5.2.2 Cylindrical Solid

The cylindrical solid consisted of a base circle with a diameter of 25 mm. This was extruded to a length of 675 mm. Figure 12 shows the solid cylinder with the dimensions. Cylindrical solid geometry had a power input of 141.89 W and an output of 149.21 W. The numerical values obtained from FLUENT® are provided in Table 4. This translated to a power per radiation area of 2738.80 W/m^2 and a power per mass of 157.46 W/kg. As compared to the theoretical value for the radiation area the efficiency of the rectangular design is 25.4 %.

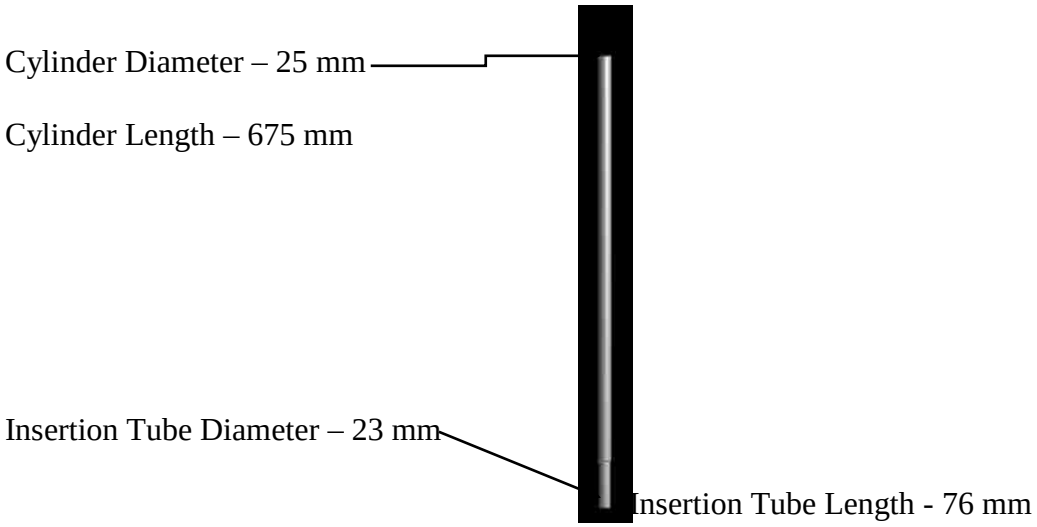

Figure 12. Schematic of solid cylinder.

Table 4. Power values for cylindrical solid.

Solid Cylinder		**Power (W)**
Insertion Tube		141.89433
Outer Radiation Surface		-149.21098
Net		-7.316649
Error	4.903559376	%

The temperature profile of the cylindrical solid is shown in Figure 13. The profile is what would be expected of a solid material. Since the only means of heat transport through the solid is conduction, the temperature is much higher near the insertion tube and drops drastically along the axis. . The insertion tube temperature is held at 700 K and the end temperature is 234 K. The temperature drops 300 K in the first third of the cylindrical solid. This can be compared to the 160 K drop along the second two-thirds.

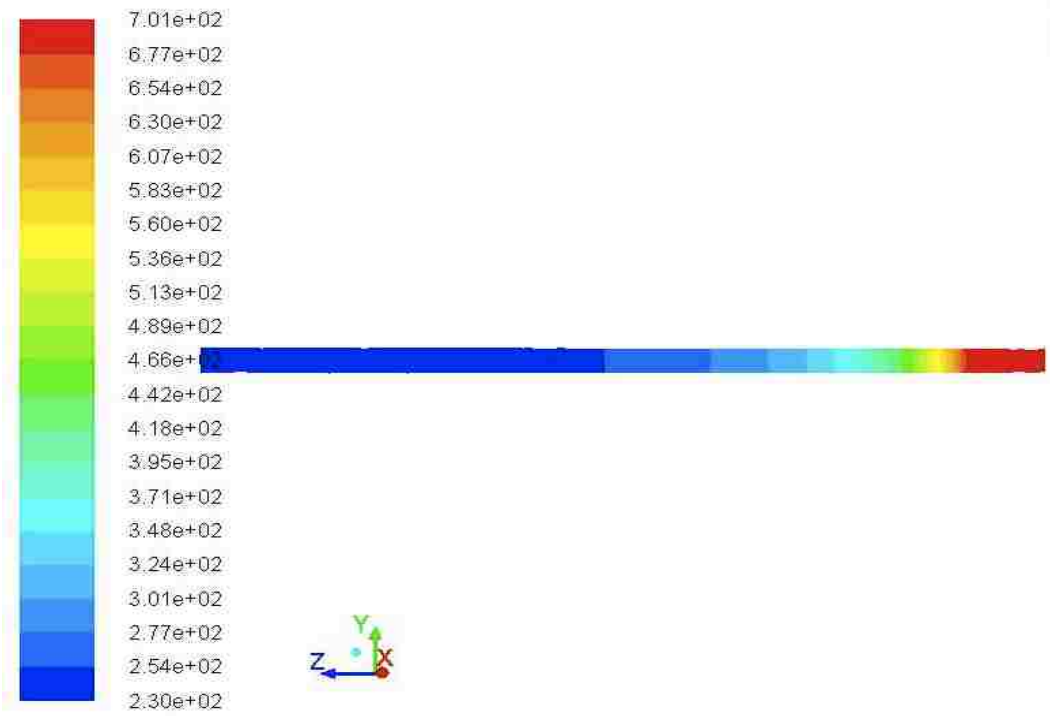

Figure 13. Temperature (K) profile of cylindrical solid.

5.2.3 Cylindrical Solid with Fins

The cylindrical solid consisted of a base circle with a diameter of 25 mm. This was integrated with the fins so as to produce the design proposed by Juhasz (1998). The fins were 25 mm in length but 2 mm in width due to limitations of the program and mesh. This was extruded to a length of 300 mm. A schematic drawing of this is shown in Figure 14. The cylindrical solid with fin geometry had a power input of 220.61 W and an output of 225.35 W. The numerical values obtained from FLUENT® are provided in Table 5. This translated to a power per radiation area of 4194.12 W/m2 and a power per mass of 384.36 W/kg. As compared to the theoretical value for the radiation area the efficiency of the rectangular design is 38.9%.

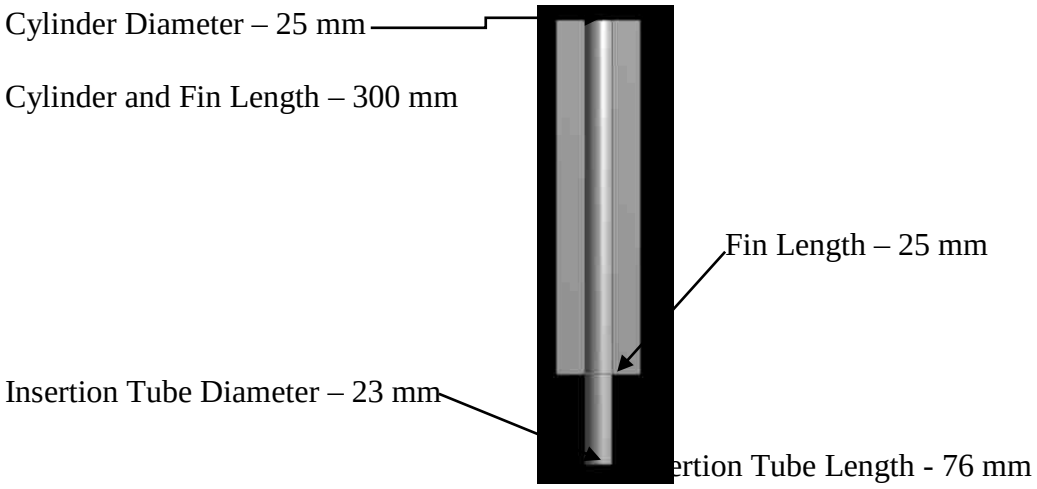

Figure 14. Schematic of cylindrical solid with fins.

Table 5. Power values for solid cylinder with fins.

Solid Cylinder with Fins		**Power (W)**
Fins		-127.2424
Insertion Tube		220.60663
Outer Radiation Surface of Pipe		-98.106845
Net		-4.7426183
Error	2.104563652	%

The temperature profile of the cylindrical solid with fins is shown in Figure 15. The profile is what would be expected of a solid material that has fins. Since the only means of heat transport through the solid is conduction, the temperature is much higher near the insertion tube. However, unlike the solid cylinder, the fins increase the surface area of radiation allowed the heat to dissipate up the solid and creates a much broader gradient. The insertion tube temperature is held at 700 K and the end temperature is 486 K. The

temperature drops 160 K in the first half of the cylindrical solid. The rest of the temperature drop, 64 K, occurs over the rest of the length.

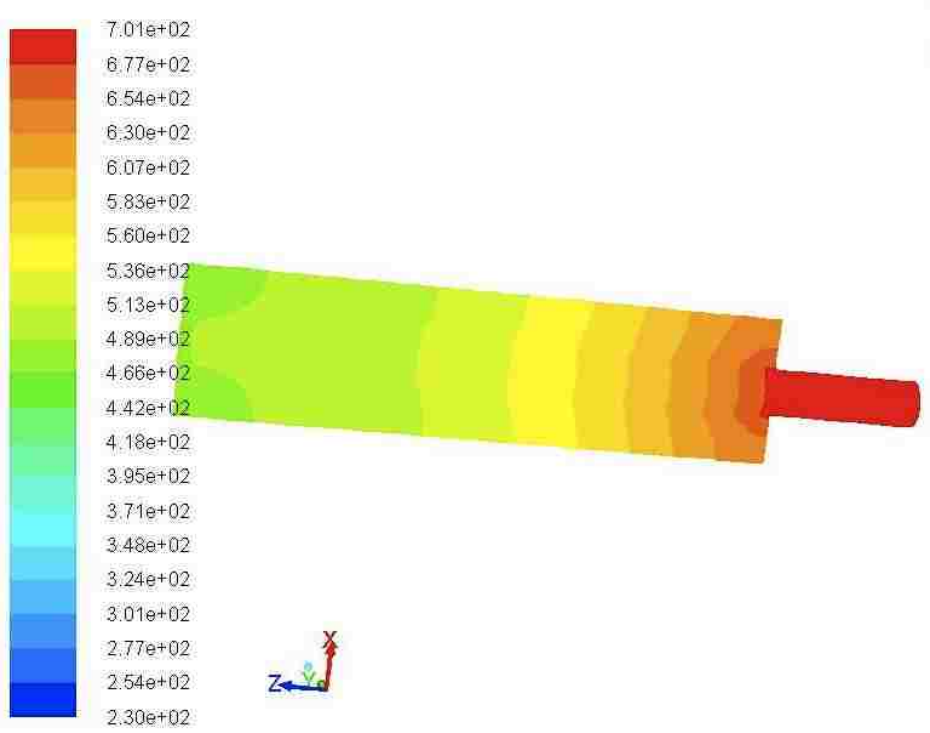

Figure 15. Temperature (K) profile of solid cylinder with fins.

5.2.4 Heat Pipe

The heat pipe outer cylinder consisted of a base circle with a diameter of 25 mm. An inner circle of 23 mm was created to make a hollow heat pipe. The wall of the heat pipe was 2 mm in width due to limitations of the program and mesh. Then end caps of 23 mm in diameter and 2 mm in thickness were created and the material merged into the existing heat pipe material. This was extruded to a length of 675 mm. This schematic is shown in Figure 16. The heat pipe geometry had a power input of 110.3788 W and an output of

110.3786 W. The numerical values obtained from FLUENT® are given in Table 6. This translated to a power per radiation area of 2053.96 W/m^2 and a power per mass of 116.48 W/kg. As compared to the theoretical value for the radiation area the efficiency of the rectangular design is 19.08%.

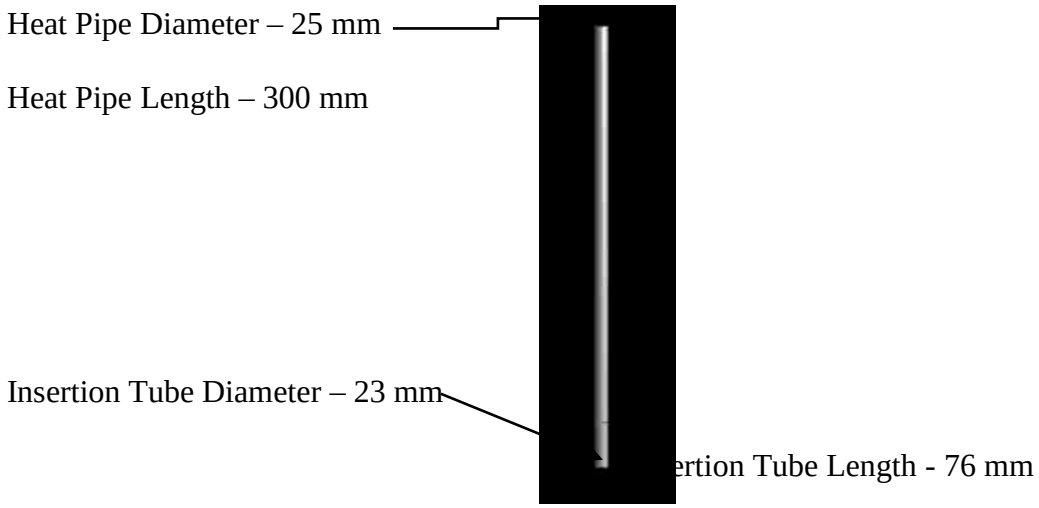

Figure 16. Schematic of heat pipe with no fin.

Table 6. Power values for heat pipe with no fin.

Heat Pipe		**Power (W)**
With Profile		
End Cap		0.85611307
Insertion tube		4.1803685
Pipe interior		105.3424
Outer Radiation Surface of Pipe		-110.37865
Net		0.000234192
Error	0.000212171	%

The temperature profile of the heat pipe is shown in Figure 17. The profile is what would be expected of a hollow material utilizing convective heat transfer inside. By using potassium to transport the heat from the insertion tube to the end cap, the temperature decrease along the heat pipe is drastically reduced. The high temperature along the length of the heat pipe assures a high heat flux from the heat pipe. The insertion tube temperature is held at 700 K and the end temperature is 617 K. The temperature drops 160 K in the first third of the heat pipe. This can be compared to the 23 K drop along the second two-thirds.

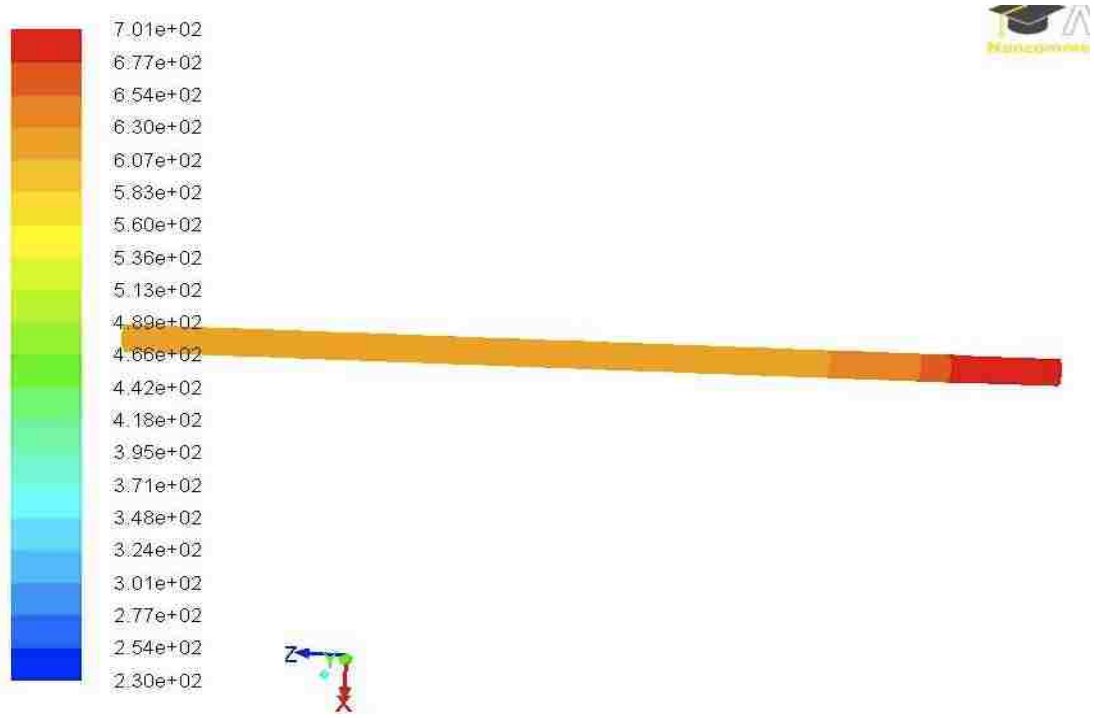

Figure 17. Temperature (K) contour of heat pipe with no fin.

5.2.5 Heat Pipe with Fins

The outer cylinder consisted of a base circle with a diameter of 25 mm. An inner circle of 23 mm was created to make a hollow heat pipe. Then end caps of 23 mm in diameter and 2 mm in thickness were created and the material merged into the existing heat pipe material. This was integrated with the fins so as to produce the design proposed by Juhasz (1998). The fins were 25 mm in width but 2 mm in thickness due to limitations of the program and mesh. This was extruded to a length of 300 mm. The schematic of this design is shown in Figure 18.

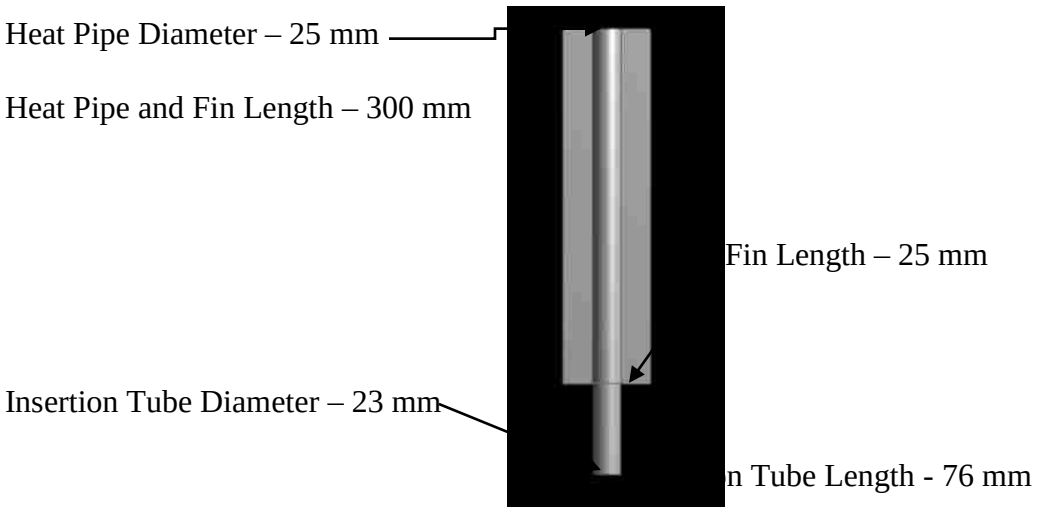

Figure 18. Schematic of heat pipe with integrated fin.

The heat pipe geometry with fin length to diameter ratio of 1.0 had a power input of 430.72 W and an output of 441.76 W. The numerical values obtained from FLUENT® are provided in Table 7. This translated to a power per radiation area of 8081.96 W/m^2 and a power per mass of 1906.60 W/kg. As compared to the theoretical value for the radiation area the efficiency of the rectangular design is 75.08%.

Table 7. Power values for heat pipe with fin.

Heat Pipe	**1.0 Ratio**	**Power (W)**
With Profile		
End Cap		-150.38675
Fin		-162.12975
Insertion tube		151.37973
Pipe interior		279.33459
Outer Radiation Surface of Pipe		-129.24197
Net		-11.04415
Error	2.500042614	%

The temperature profile of the heat pipe is shown in Figure 19. The insertion tube temperature is held at 700 K and the end temperature is 425 K. The temperature drops only 200 K along the majority of the heat pipe. The profile is what would be expected of a hollow material utilizing convective heat transfer inside. By using potassium to transport the heat from the insertion tube to the end cap, the temperature decreases along the heat pipe is drastically reduced. The high temperature along the length of the heat pipe assures a high heat flux from the heat pipe

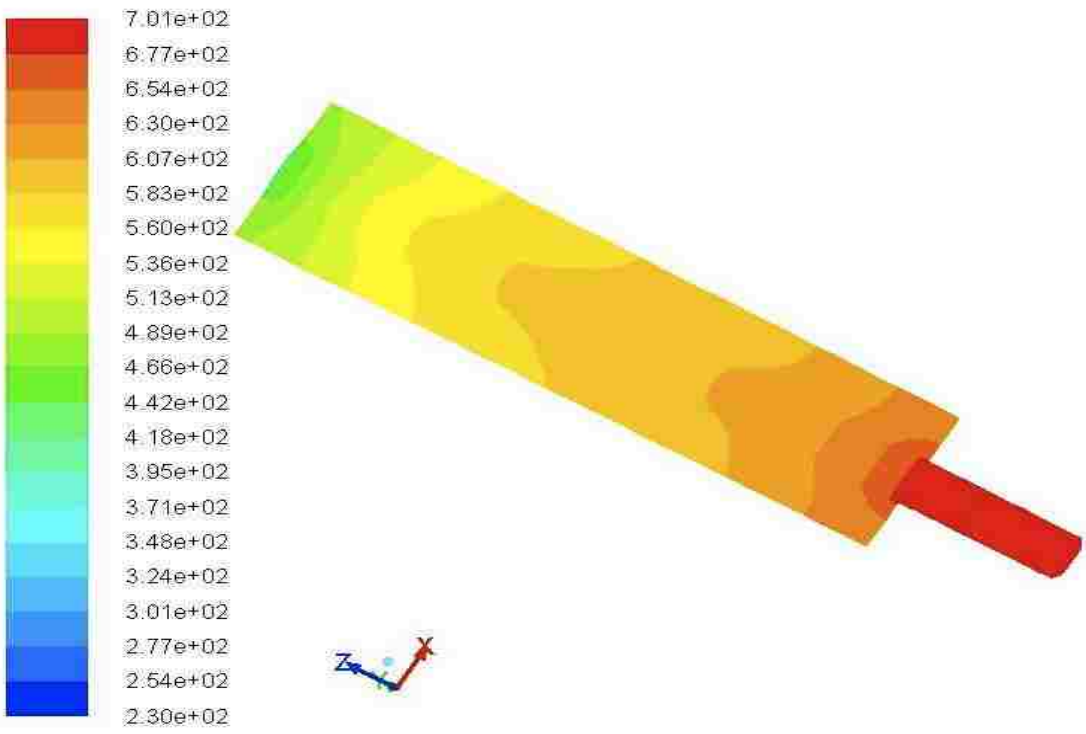

Figure 19. Temperature (K) contour of heat pipe with 1.0 fin width to pipe length ratio.

5.2.6 Results and Discussions of Parametric Comparison

The following images are the temperature contours, shown in Figure 20, of the simulation. It can be noted that by introspection that the heat pipe with fins geometry out performs the other geometries. This geometry provides the highest temperature difference along the length. This in turn provides the greatest ability for heat removal.

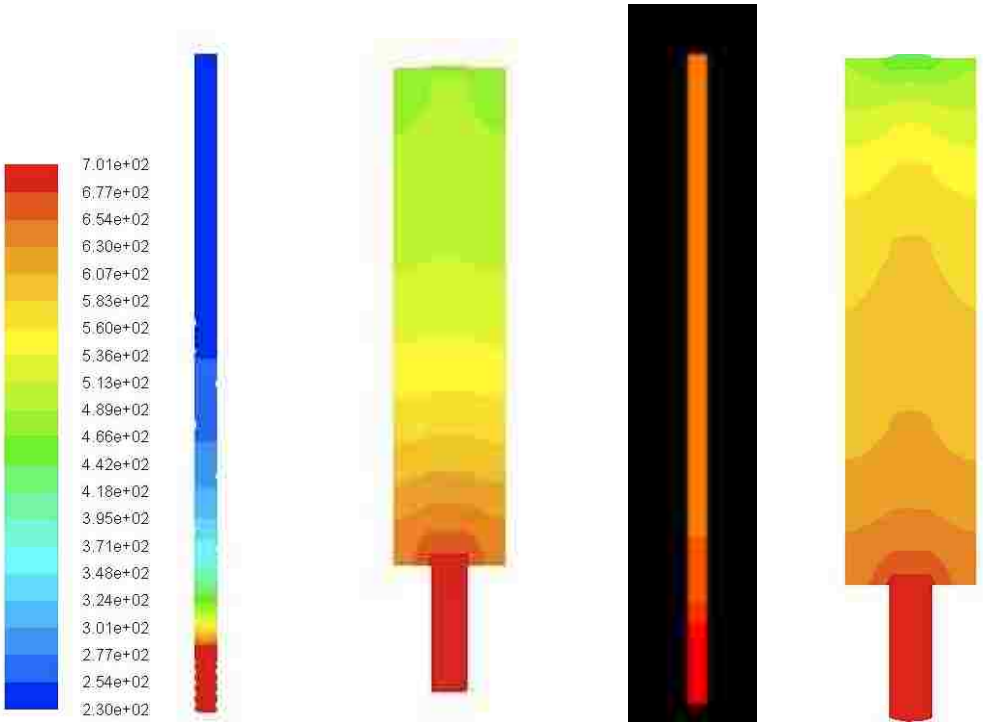

Figure 20. Temperature (K) comparison of various geometries. (a) Cylindrical Solid (b) Cylindrical Solid with fins (c) Heat Pipe and (d) Heat Pipe with fins.

By comparing the results of the various geometries with similar radiation areas we can ascertain the best design for a radiator system. This is achieved by comparing the power output per unit mass and the power output per unit radiation area. The design chosen was a balance between the maximum amount of power per unit mass and maximum power per unit area. This should optimize the power output while reducing the weight of a system. In Table 8 the values of the various geometries considered are listed along with the power per unit area, power per unit mass, theoretical output, and efficiency. Figure 21 shows a bar graph of the power per unit area for the different geometries. From this figure it is clear to find that the heat pipe with fins is the best performer. In Figure 22, which compares the power per unit mass, the heat pipe with fins also far exceeds the other designs. These results are expected as the heat pipe allows the greatest radiation area but also allows for better

heat transfer along the heat pipe due to the working fluid being able to move along the interior of the pipe, thus keeping the temperature along the pipe higher.

Table 8. Comparison of power per unit area, power per unit mass, and efficiency of various geometries.

Geometry	Output W	Area m^2	Mass kg	Power/Area W/m^2	Power/Mass W/kg	Theoretical Power Output W	Efficiency %
Rectangular Solid	157.00	0.05	0.95	3140.00	165.68	538.23	29.17
Cylindrical Solid	149.21	0.05	0.95	2984.20	157.46	538.23	27.72
Cylindrical Solid with Fins	225.35	0.05	0.59	4507.00	384.36	538.23	41.87
Heat Pipe	373.29	0.05	0.29	7465.80	1284.99	538.23	69.36
Heat Pipe with Fins	441.76	0.05	0.23	8835.20	1906.60	538.23	82.08

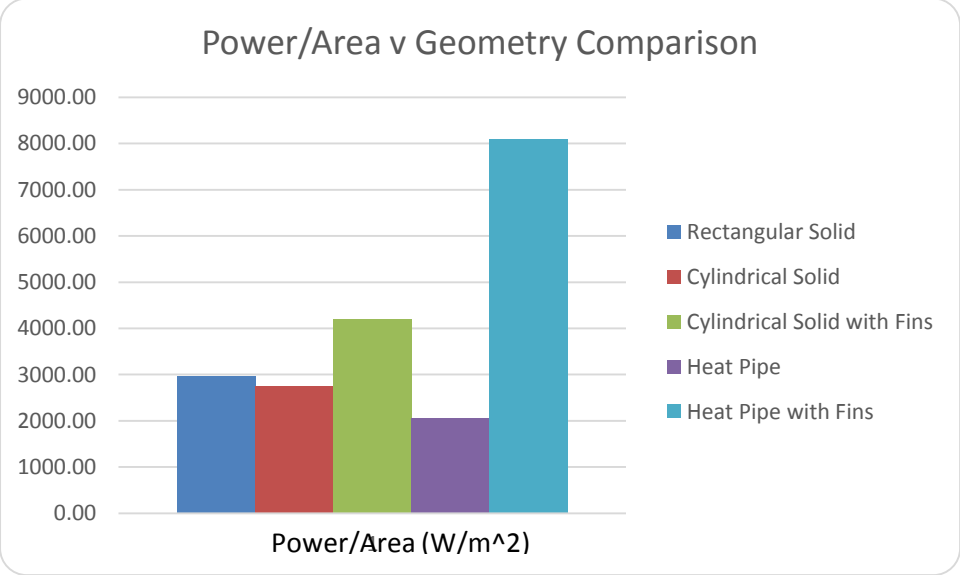

Figure 21. Comparison of power per unit area for various geometries.

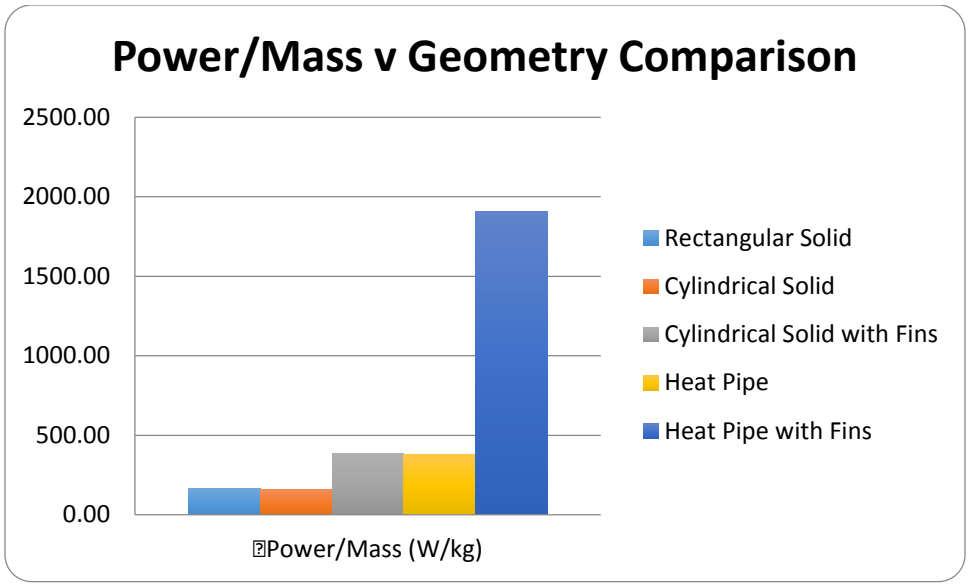

Figure 22. Comparison of power per unit mass various geometries.

5.3 Fin Length Comparison with Wick Profile

Once the heat pipe design was determined to be the best selection, then determining the optimal fin length was done to optimize the design. The fin length for each design was determined by looking at a ratio of fin length to outer pipe diameter. The ratios were arbitrarily selected at regular intervals increasing by 0.25 from 0 to 1.5. The power output per unit area and the power output per unit mass were analyzed. That combined with the calculated efficiency was used to ascertain the best selection for the design.

5.3.1 Ratio of 0.25

The outer cylinder consisted of a base circle with a diameter of 25 mm. An inner circle of 23 mm was created to make a hollow heat pipe. Then end caps of 23 mm in diameter and 2 mm in thickness were created and the material merged into the existing heat pipe material. The fins were 6.25 mm in width but 2 mm in thickness due to limitations of the

program and mesh. This was extruded to a length of 300 mm. The schematic of this design is shown in Figure 23.

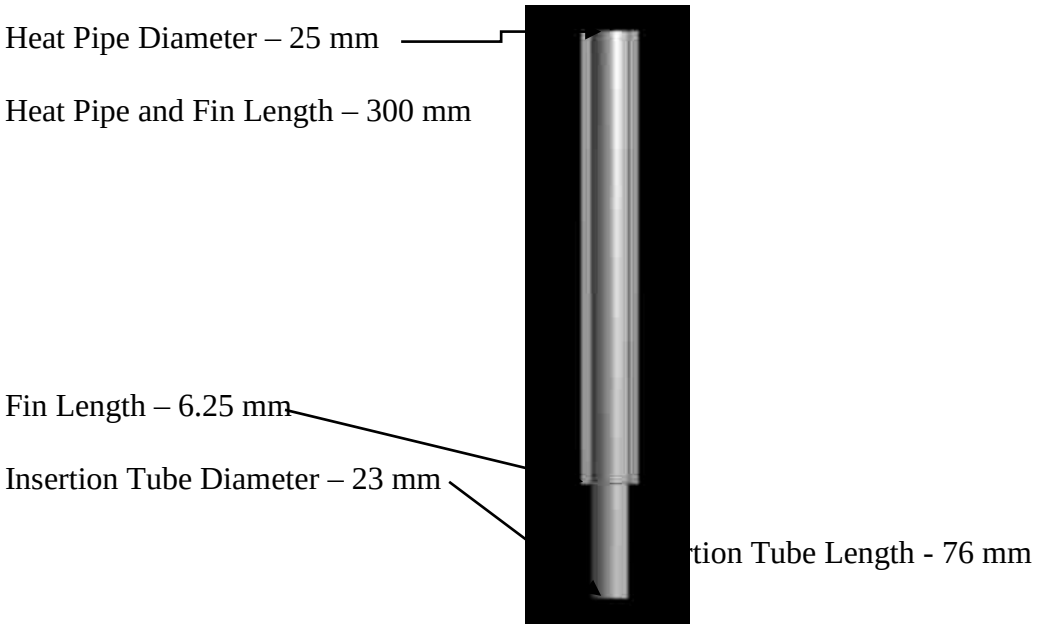

Figure 23. Schematic of heat pipe with integrated fin using a fin ratio of 0.25.

The heat pipe geometry with fin length to heat pipe diameter ratio of 0.25 had a power input of 336.36 W and an output of 339.36 W. This translated to a power per radiation area of 10608.32 W/m^2 and a power per mass of 1991.55 W/kg. The numerical data is provided in Table 9. As compared to the theoretical value for the radiation area the efficiency of the rectangular design is 98.5 %.

Table 9. Power values for heat pipe with ratio of 0.25.

Heat Pipe	**0.25 Ratio**	**Power (W)**
End Cap		-144.63903
Fins		-52.670822
Insertion Tube		124.37996
Pipe Interior		211.98478
Outer Radiation Surface of Pipe		-142.05378
Net		-2.998892
Error	0.883681019	%

The temperature profile of the heat pipe is shown in Figure 24. The insertion tube temperature is held at 700 K and the end temperature is 425 K. The temperature drops 210 K along the majority of the heat pipe to 490 K. The profile is what would be expected of a hollow material utilizing convective heat transfer inside. The high temperature along the length of the heat pipe assures a high heat flux from the heat pipe.

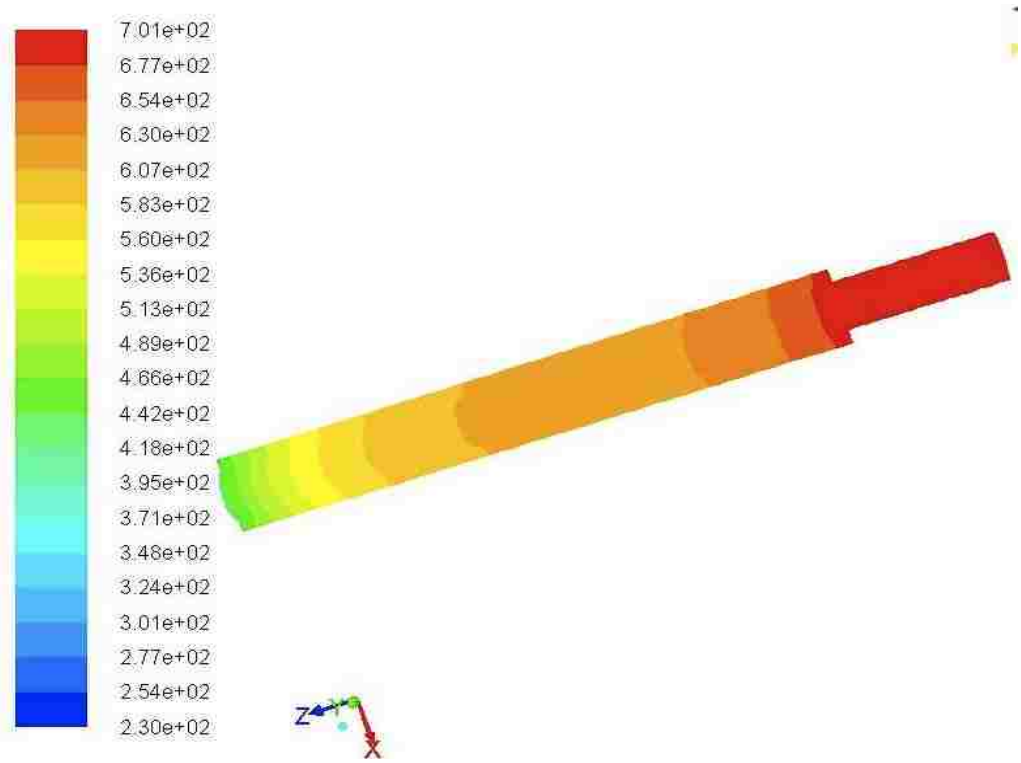

Figure 24. Temperature (K) contour of heat pipe with 0.25 fin width to pipe length ratio.

5.3.2 Ratio of 0.5

The outer cylinder consisted of a base circle with a diameter of 25 mm. An inner circle of 23 mm was created to make a hollow heat pipe. Then end caps of 23 mm in diameter and 2 mm in thickness were created and the material merged into the existing heat pipe material. The fins were 12.5 mm in width but 2 mm in thickness due to limitations of the program and mesh. This was extruded to a length of 300 mm. The schematic of this design is shown in Figure 25.

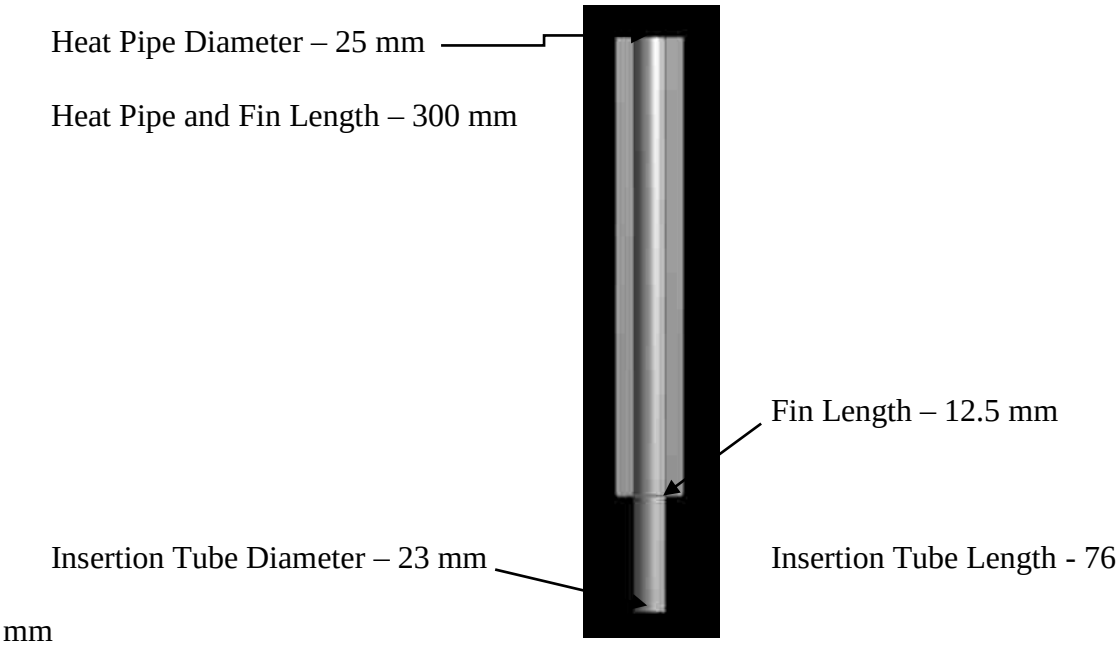

Figure 25. Schematic of heat pipe with integrated fin using a fin ratio of 0.5.

The heat pipe geometry with fin length to diameter ratio of 0.50 had a power input of 380.75 W and an output of 382.13 W. This translated to a power per radiation area of 9659.50 W/m^2 and a power per mass of 2028.29 W/kg. As compared to the theoretical value for the radiation area the efficiency of the rectangular design is 89.7%. The numerical data is provided in Table 10.

Table 10. Power values for heat pipe with ratio of 0.5.

Heat Pipe	**0.5 Ratio**	**Power (W)**
End Cap		-155.52128
Fins		-92.230587
Insertion Tube		134.75903
Pipe Interior		245.98682
Outer Radiation Surface of Pipe		-134.3784
Net		-1.384417
Error	0.362289282	%

The temperature profile of the heat pipe is shown in Figure 26. The insertion tube temperature is held at 700 K and the end temperature is 425 K. The temperature drops only 214 K along the majority of the heat pipe. The temperature gradient is slightly less than the 0.25 ratio gradient varying by only 4 K.

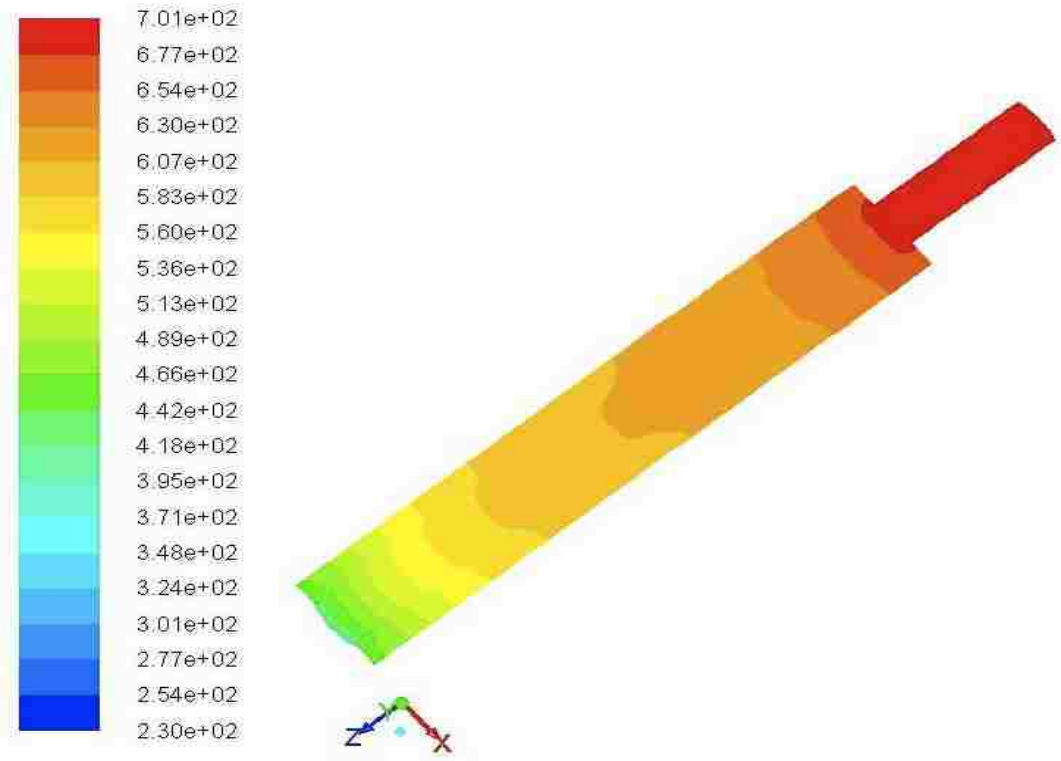

Figure 26. Temperature (K) contour of heat pipe with 0.5 fin width to pipe length ratio.

5.3.3 Ratio of 0.75

The outer cylinder consisted of a base circle with a diameter of 25 mm. An inner circle of 23 mm was created to make a hollow heat pipe. Then end caps of 23 mm in diameter and 2 mm in thickness were created and the material merged into the existing heat pipe material. The fins were 18.75 mm in width but 2 mm in thickness due to limitations of the program and mesh. This was extruded to a length of 300 mm. The schematic of this design is shown in Figure 27.

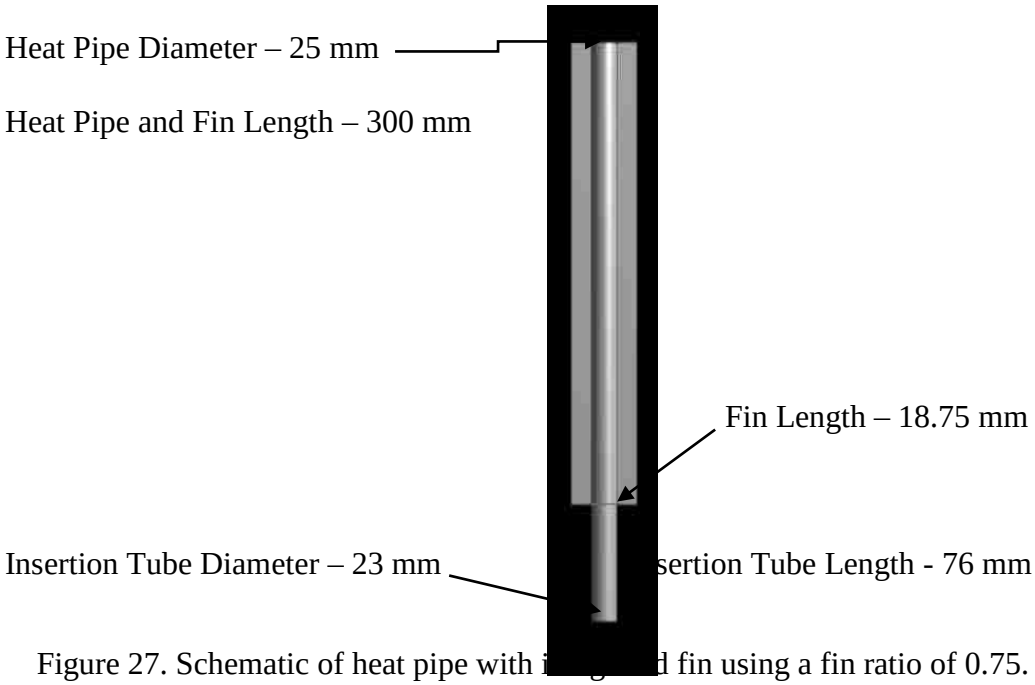

Figure 27. Schematic of heat pipe with i d fin using a fin ratio of 0.75.

The heat pipe geometry with fin length to diameter ratio of 0.75 had a power input of 404.86 W and an output of 406.96 W. This translated to a power per radiation area of 8693.87 W/m^2 and a power per mass of 1949.04 W/kg. The numerical data is provided in Table 11. As compared to the theoretical value for the radiation area the efficiency of the rectangular design is 80.8%.

Table 11. Power values for heat pipe with ratio of 0.75**.**

Heat Pipe	**0.75 Ratio**	**Power (W)**
With Profile		
End Cap		-147.84795
Fins		-125.36772
Insertion Tube		143.03131
Pipe Interior		261.83097
Outer Radiation Surface of Pipe		-133.74557
Net		-2.0989544
Error	0.51576273	%

The temperature profile of the heat pipe is shown in Figure 28. The insertion tube temperature is held at 700 K and the end temperature is 415 K. The temperature drops only 206 K along the majority of the heat pipe. The end cap temperature is less than that of the 0.25 or 0.5 ratio designs which is to be expected due to the increase in fin size.

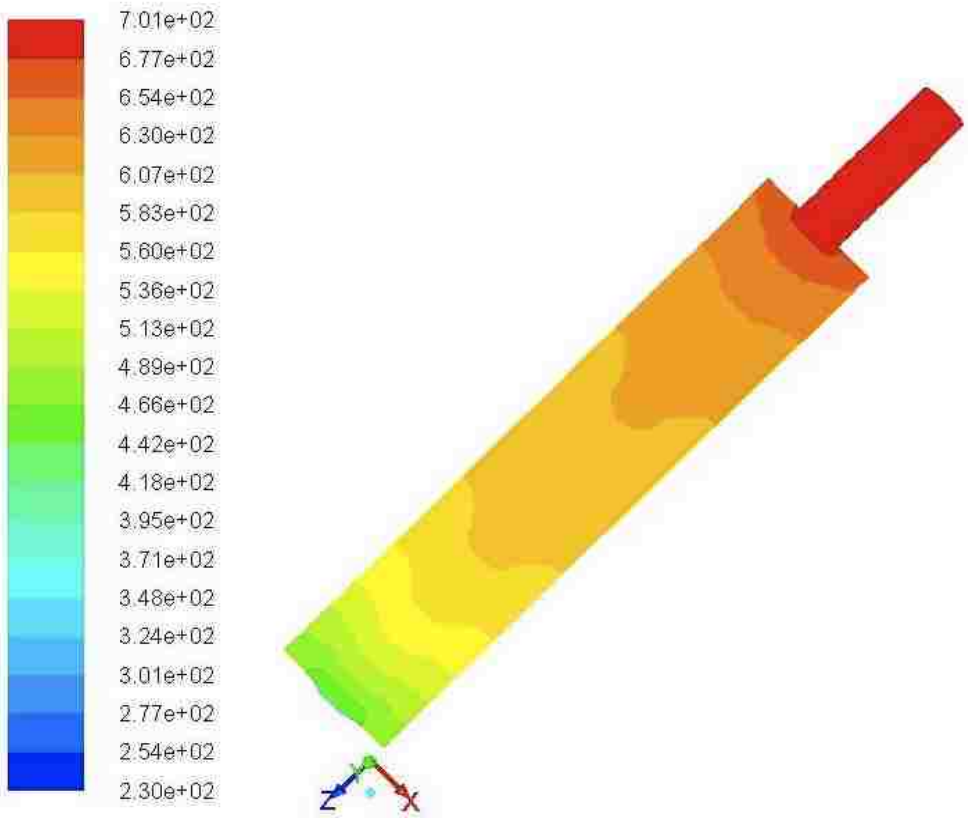

Figure 28. Temperature (K) contour of heat pipe with 0.75 fin width to pipe length ratio.

5.3.4 Ratio of 1.25

The outer cylinder consisted of a base circle with a diameter of 25 mm. An inner circle of 23 mm was created to make a hollow heat pipe. Then end caps of 23 mm in diameter and 2 mm in thickness were created and the material merged into the existing heat pipe material. The fins were 31.25 mm in width but 2 mm in thickness due to limitations of the program and mesh. This was extruded to a length of 300 mm. The schematic of this design is shown in Figure 29.

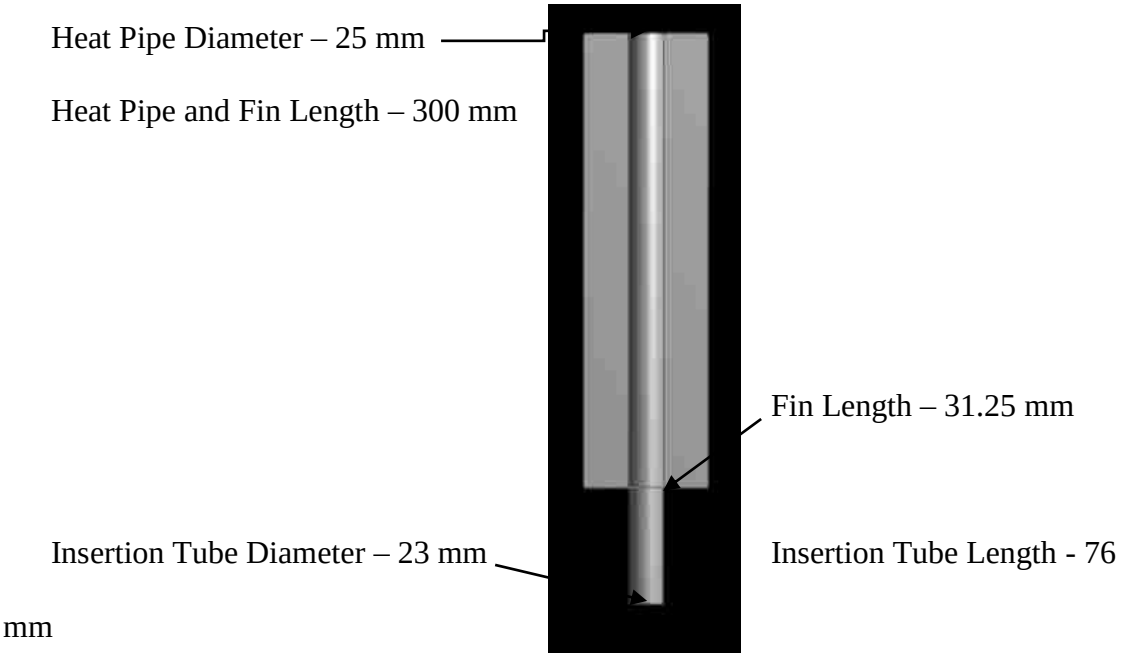

Figure 29. Schematic of heat pipe with integrated fin using a fin ratio of 1.25.

The heat pipe geometry with fin length to diameter ratio of 1.25 had a power input of 475.31 W and an output of 477.17 W. This translated to a power per radiation area of 7669.08 W/m^2 and a power per mass of 1892.78 W/kg. The numerical data is provided in Table 12. As compared to the theoretical value for the radiation area the efficiency of the rectangular design is 71.2 %.

Table 12. Power values for heat pipe with ratio of 1.25.

Heat Pipe	**1.25 Ratio**	**Power (W)**
With Profile		
End Cap		-167.13698
Fins		-187.32096
Insertion Tube		158.96513
Pipe Interior		316.3428
Outer Radiation Surface of Pipe		-122.71281
Net		-1.86282
Error	0.390388556	%

The temperature profile of the heat pipe is shown in Figure 30. The insertion tube temperature is held at 700 K and the end temperature is 400 K. The temperature drops by 225 K along the majority of the heat pipe. The increase in fin length is now having a noticeable effect in that the temperature along the radiation surface is decreasing at faster rate than the previous designs.

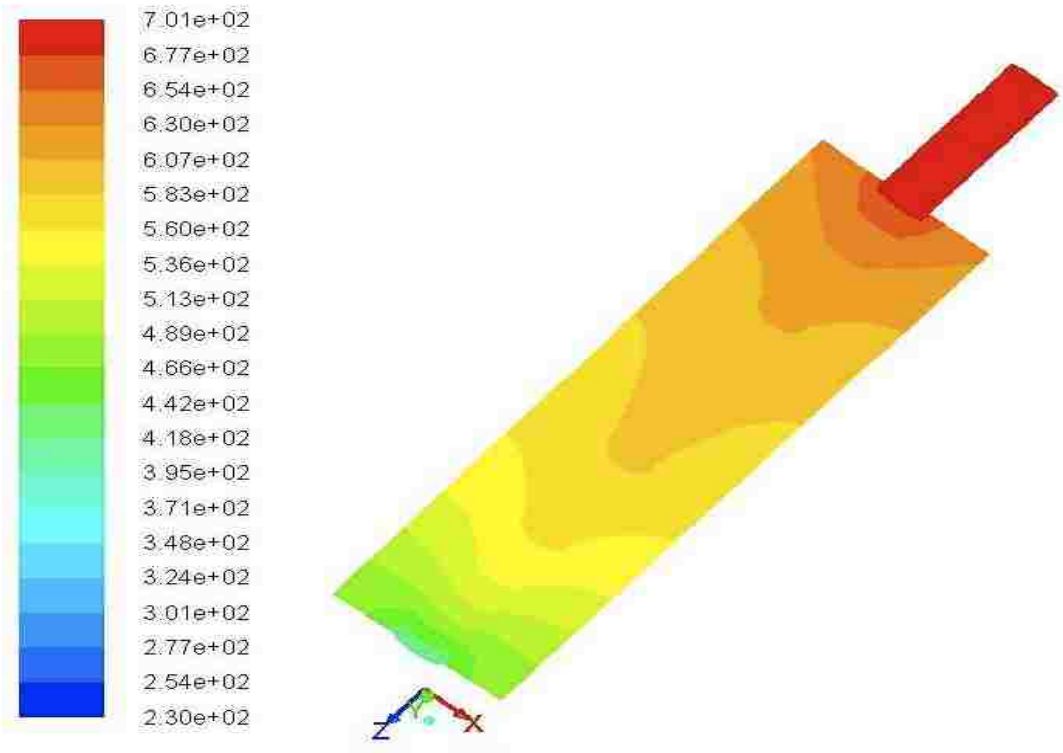

Figure 30. Temperature (K) contour of heat pipe with 0.75 fin width to pipe length ratio.

5.3.5 Ratio of 1.5

The outer cylinder consisted of a base circle with a diameter of 25 mm. An inner circle of 23 mm was created to make a hollow heat pipe. Then end caps of 23 mm in diameter and 2 mm in thickness were created and the material merged into the existing heat pipe material. The fins were 37.5 mm in width but 2 mm in thickness due to limitations of the program and mesh. This was extruded to a length of 300 mm. The schematic of this design is shown in Figure 31.

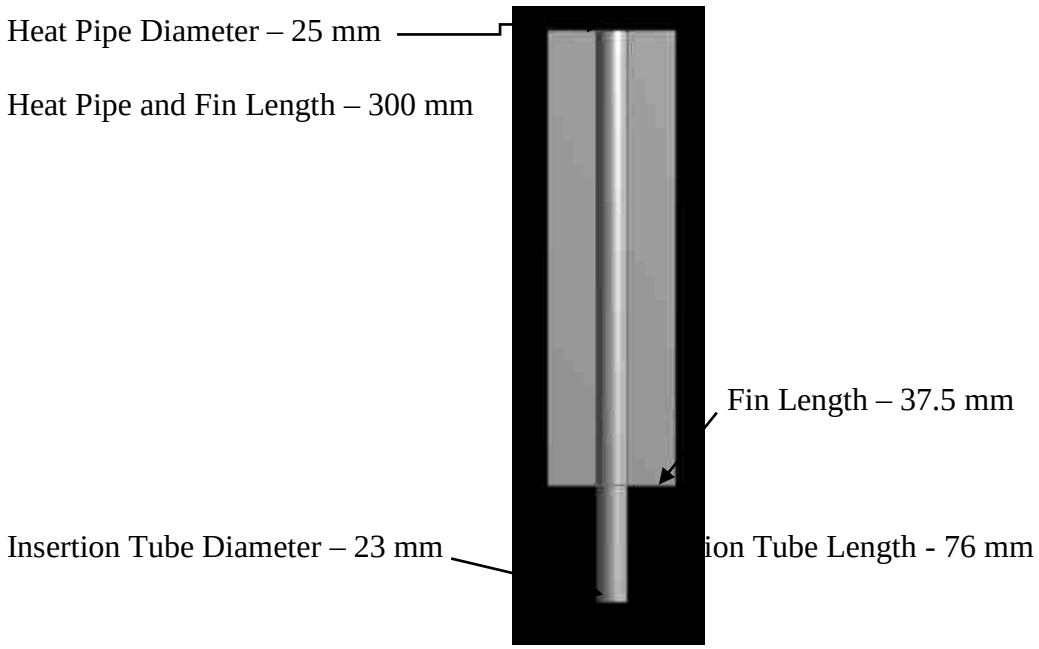

Figure 31. Schematic of heat pipe with integrated fin using a fin ratio of 1.5.

The heat pipe geometry with fin length to diameter ratio of 1.50 had a power input of 492.43 W and an output of 498.31 W. This translated to a power per radiation area of 7142.18 W/m^2 and a power per mass of 1822.64 W/kg. As compared to the theoretical value for the radiation area the efficiency of the rectangular design is 66.3%. The numerical data is provided in Table 13.

Table 13. Power values for heat pipe with ratio of 1.5**.**

Heat Pipe	**1.5 Ratio**	**Power (W)**
End Cap		-165.90965
Fins		-212.78896
Insertion Tube		164.57774
Pipe Interior		332.38892
Outer Radiation Surface of Pipe		-119.6151
Net		-1.34705
Error	0.270321681	%

The temperature profile of the heat pipe is shown in Figure 32. The insertion tube temperature is held at 700 K and the end temperature is 400 K. The temperature drops again by 225 K along the majority of the heat pipe. This design has the most rapid temperature decrease among the heat pipe designs. This is expected as the increase in fin size created a larger surface area for radiation.

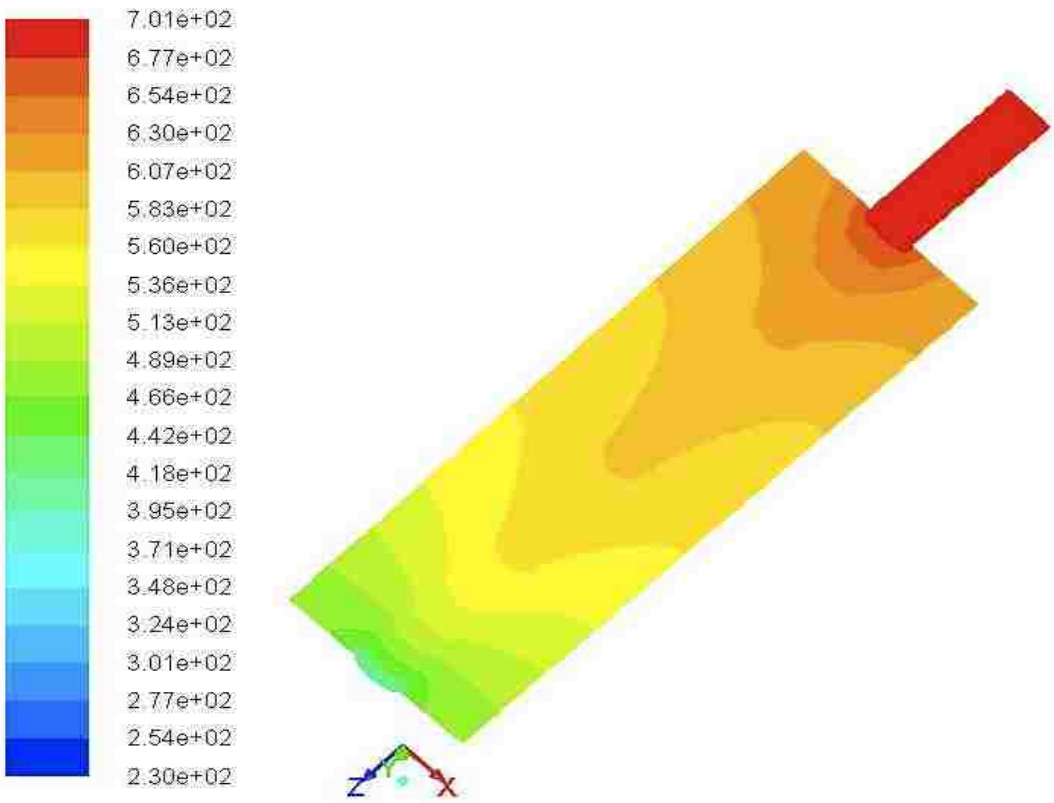

Figure 32. Temperature (K) contour of heat pipe with 1.5 fin width to pipe length ratio.

5.3.6 Results and Discussions of Fin Length Comparison with Profile Data

The following results shown in Figure 33 are the temperature contours of the simulations comparing fin ratios. From the temperature contour plots it is observed that the temperature decreases more rapidly as the fin length is increased. This combined with the increase in mass due to general size demonstrates that a smaller fin length is reasonable and preferable.

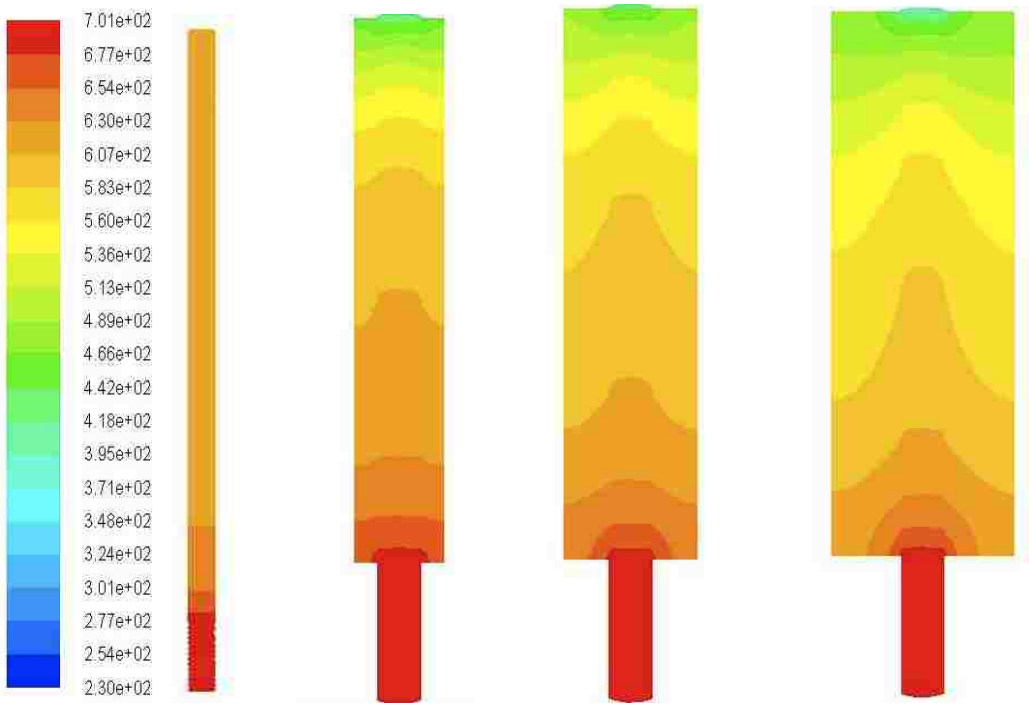

Figure 33. Temperature (K) comparison of various fin lengths and wick profile data. (a) Heat Pipe (b) Heat Pipe with ratio of 0.5 (c) Heat Pipe with ratio of 1.0 and (d) Heat Pipe with ratio of 1.5.

The following data in table, Table 14, shows that maximum heat transfer per unit area and per unit mass occurs at a fin width to pipe diameter of 0.5 ratio. It is also of note that the efficiency decreases as the width of the fins increase. This decrease in efficiency is significant, at 32.2 % decrease over the change in fin width, and must be considered. Since the optimal fin width to pipe diameter is on the lower end the efficiency is nearly 90% thus the efficiency is higher than would be expected. The power per unit area and power per unit mass were shown as a function of fin ratio in Figure 34. This data proved somewhat inconclusive as the values for the ratios of 0.25 and 0.5 were extremely close. For this reason the data was put into a bar chart to compare power per unit area, shown in Figure 35, and power per unit mass, shown in Figure 36, in order to better compare the data.

Table 14. Comparison of power per unit area and power per unit mass for various fin width to pipe diameter for design including wick profile data.

Geometry	Output (W)	Area m^2	Mass kg	Power/Area W/m^2	Power/ Mass W/kg	Theoretical Power Output W	Efficiency %
Heat Pipe	110.38	0.05374	0.9476	2053.96	116.48	578.49	19.08
Heat Pipe Ratio 0.25	339.36	0.03199	0.1704	10608.32	1991.55	344.36	98.55
Heat Pipe Ratio 0.50	382.13	0.03956	0.1884	9659.50	2028.29	425.85	89.73
Heat Pipe Ratio 0.75	406.96	0.04681	0.2088	8693.87	1949.04	503.89	80.76
Heat Pipe Ratio 1.0	441.76	0.05466	0.2317	8081.96	1906.60	588.39	75.08
Heat Pipe Ratio 1.25	477.17	0.06222	0.2521	7669.08	1892.78	669.77	71.24
Heat Pipe Ratio 1.5	498.31	0.06977	0.2734	7142.18	1822.64	751.04	66.35

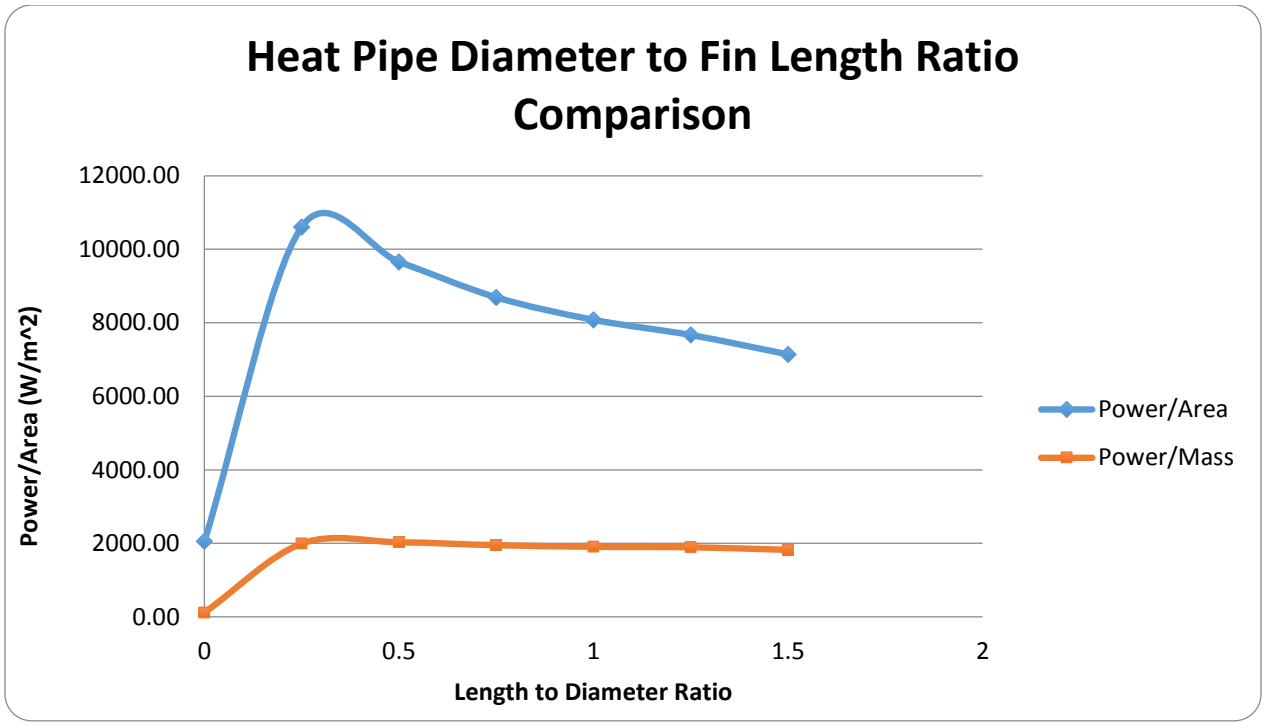

Figure 34. Comparison of power per unit area and power per unit mass for various fin width to pipe diameter for design including wick profile data.

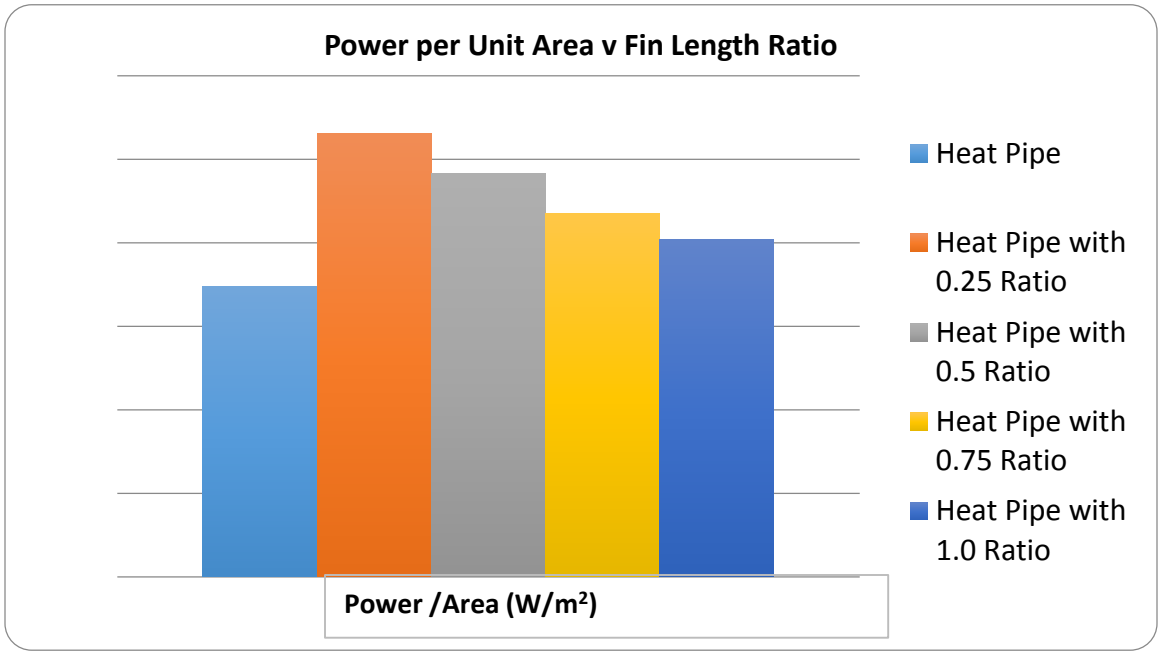

Figure 35. Power per unit area for various fin ratios for design including wick profile data.

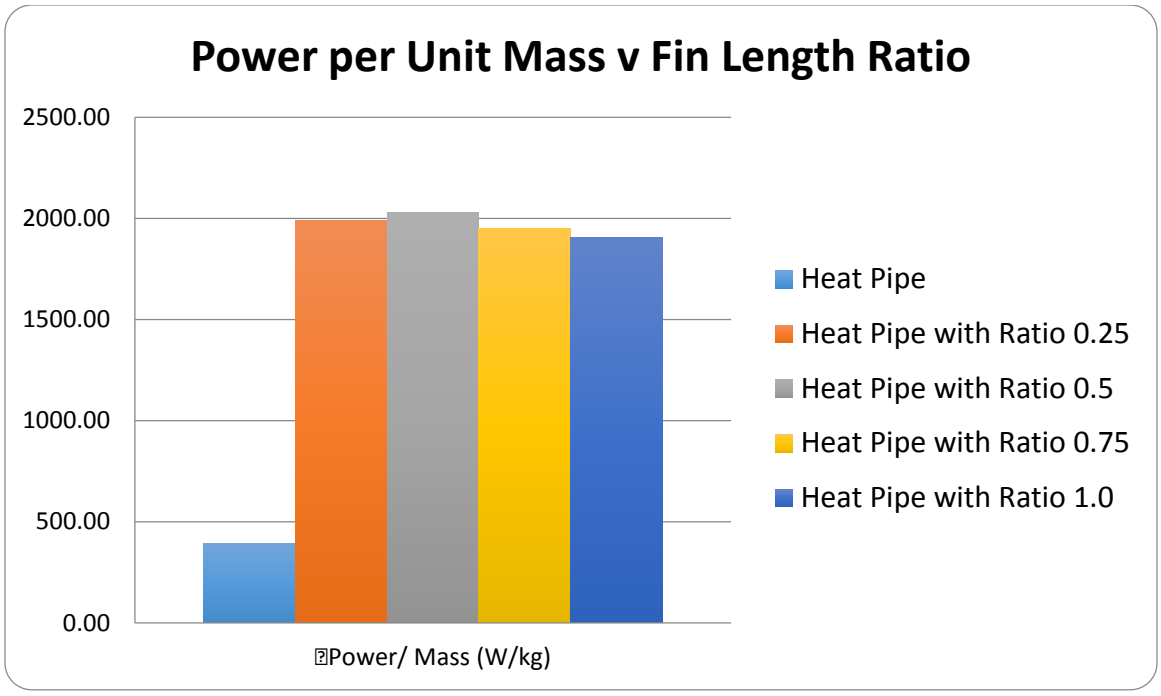

Figure 36. Power per unit mass comparison for various fin ratios for design including wick profile data.

5.4 Heat Pipe Design for Fin Width Comparison without Profile Correction

Another area of interest was how much effect did the wick profile data have on the ultimate result of the simulation. This was of interest for two reasons. First, it validates that the equivalent wick performance study was necessary since the wick structure was not being modeled in this design. Second, it determines if there is a need to at some point numerically model various wick structures due the impact on the overall design. The same designs, varying of fin ratios, as above were simulated and power outputs determined.

5.4.1 Heat Pipe with No Fin

The heat pipe geometry no fin had a power input of 1.24 W and an output of 1.24 W. This translated to a power per radiation area of 23.07 W/m^2 and a power per mass of 1.31

W/kg. As compared to the theoretical value for the radiation area the efficiency of the rectangular design is 0.21 %. The raw numerical data obtained from FLUENT® used to determine the above values is provided in Table 15.

Table 15. Power values for heat pipe with no fin and no wick profile boundary condition.

Heat Pipe		**Power (W)**
End Cap		0
Fins		0
Insertion Tube		1.2375902
Pipe Interior		0
Outer Radiation Surface of Pipe		-1.2378148
Net		-0.00022468
Error	0.018151307	%

The temperature profile of the heat pipe is shown in Figure 37. The insertion tube temperature is held at 700 K and the end temperature is 230 K. The temperature drops instantaneously due to the heat transfer only as a function of conduction down the heat pipe.

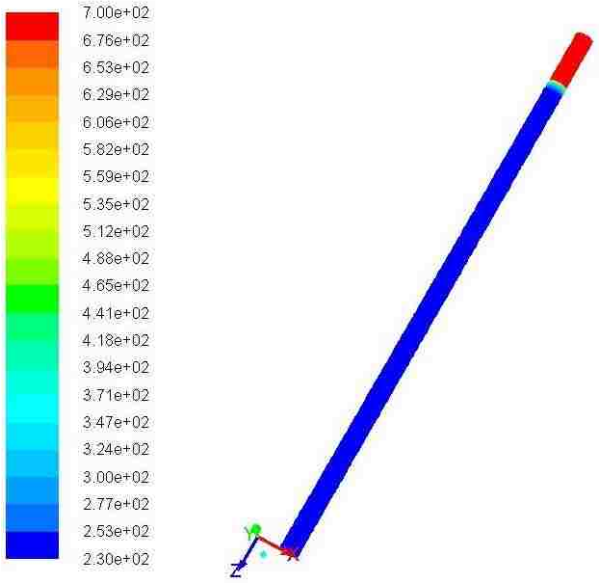

Figure 37. Temperature (K) profile of heat pipe with no fin and no wick profile boundary condition.

5.4.2 Ratio of 0.25

The heat pipe geometry with fin length to heat pipe diameter ratio of 0.25 had a power input of 102.02 W and an output of 104.36 W. This translated to a power per radiation area of 3262.27 W/m^2 and a power per mass of 612.44 W/kg. As compared to the theoretical value for the radiation area the efficiency of the rectangular design is 30.3 %. The raw numerical data obtained from FLUENT® used to determine the above values is provided in Table 16.

Table 16. Power values for heat pipe with ratio of 0.25 and no wick profile boundary condition.

Heat Pipe	**0.25 Ratio**	**Power (W)**
End Cap		-0.4727065
Fins		-27.491296
Insertion Tube		102.02179
Pipe Interior		0
Outer Radiation Surface of Pipe		-76.399496
Net		-2.3417085
Error	2.243800307	%

The temperature profile of the heat pipe is shown in Figure 38. The insertion tube temperature is held at 700 K and the end temperature is 427 K. The temperature drops 220 K along the first half of the heat pipe. This gradient is more gradual than that of the heat pipe with the working fluid boundary conditions.

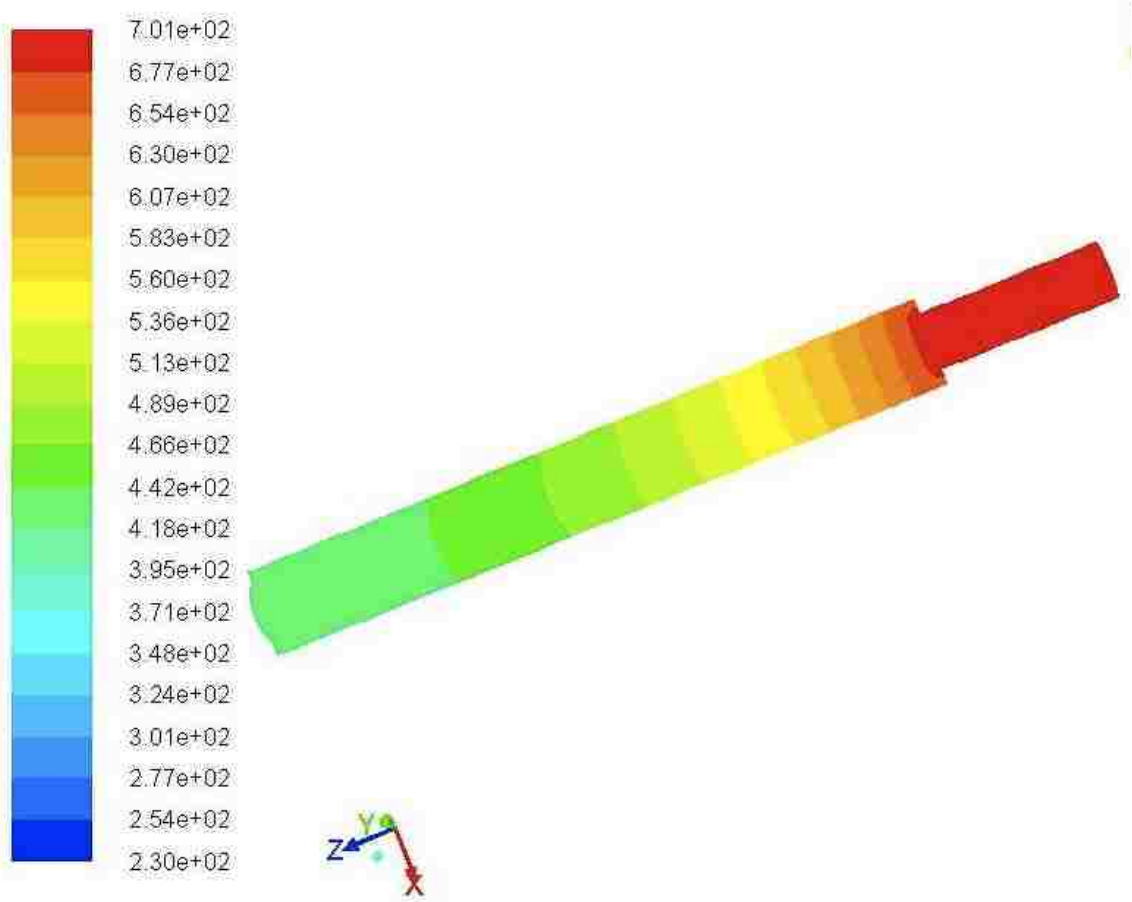

Figure 38. Temperature (K) profile of heat pipe with 0.25 ratio and no wick profile boundary condition.

5.4.3 Ratio of 0.5

The heat pipe geometry with fin length to diameter ratio of 0.50 had a power input of 118.15 W and an output of 122.55W. This translated to a power per radiation area of 3097.83 W/m^2 and a power per mass of 650.48 W/kg. The raw numerical data obtained from FLUENT® used to determine the above values is provided in Table 17. As compared to the theoretical value for the radiation area the efficiency of the rectangular design is 28.8 %.

Table 17. Power values for heat pipe with ratio of 0.5 and no wick profile boundary condition.

Heat Pipe	**0.5 Ratio**	**Power (W)**
End Cap		-0.46094671
Fins		-48.857798
Insertion Tube		118.14722
Pipe Interior		0
Outer Radiation Surface of Pipe		-73.231041
Net		-4.40256571
Error	3.592471161	%

The temperature profile of the heat pipe is shown in Figure 39. The insertion tube temperature is held at 700 K and the end temperature is 423 K. The temperature drops only 200 K along the heat pipe. The profile is what would be expected of a hollow material. Since there is no compensation for the wick effect the heat transfer along the heat pipe behaves much like that of the solid materials. The majority of the heat transfer occurs in the first two thirds of the heat pipe and the rest of the pipe has a relatively low temperature causing a decreased temperature gradient.

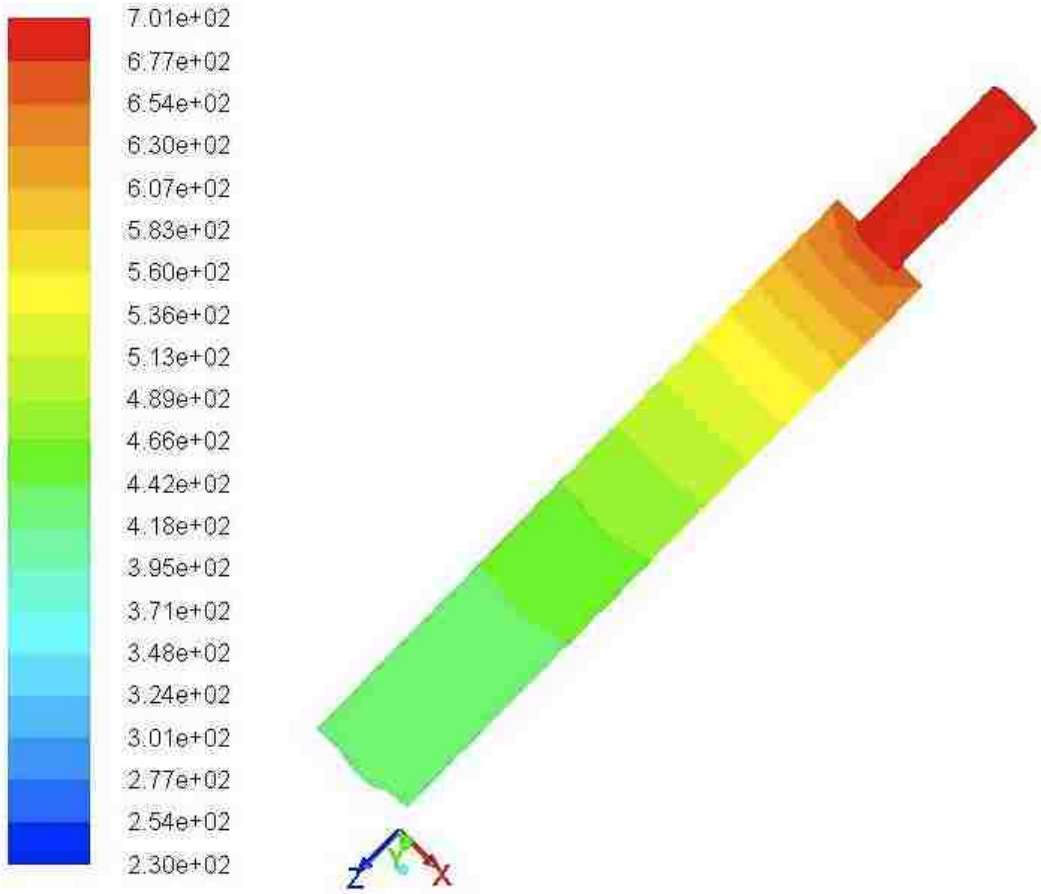

Figure 39. Temperature (K) profile of heat pipe with 0.5 ratio and no wick profile boundary condition.

5.4.4 Ratio of 0.75

The heat pipe geometry with fin length to diameter ratio of 0.75 had a power input of 130.55 W and an output of 137.3 W. This translated to a power per radiation area of 2933.13 W/m^2 and a power per mass of 657.57 W/kg. The raw numerical data obtained from FLUENT® used to determine the above values is provided in Table 18. As compared to the theoretical value for the radiation area the efficiency of the rectangular design is 27.2 %.

Table 18. Power values for heat pipe with ratio of 0.75 and no wick profile boundary condition.

Heat Pipe	**0.75 Ratio**	**Power (W)**
End Cap		-0.4449315
Fins		-65.462685
Insertion Tube		130.54867
Pipe Interior		0
Outer Radiation Surface of Pipe		-71.397853
Net		-6.7567954
Error	4.920995081	%

The temperature profile of the heat pipe is shown in Figure 40. The insertion tube temperature is held at 700 K and the end temperature is 419 K. The temperature drops 210 K along the first half of the heat pipe. As the fin length gets longer the end cap temperature is dropping more rapidly for each case and the area where the temperature is at its lowest is growing to be a larger portion of the heat pipe.

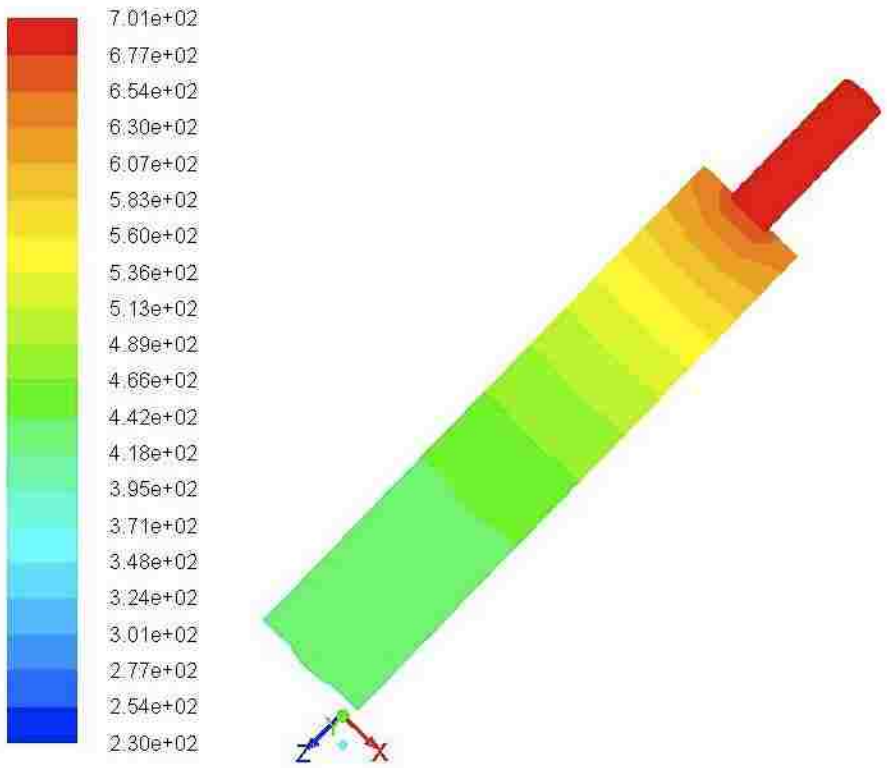

Figure 40. Temperature (K) profile of heat pipe with 0.75 ratio and no wick profile boundary condition.

5.4.5 Ratio of 1.0

The heat pipe geometry with fin length to heat pipe diameter ratio of 1.0 had a power input of 144.89 W and an output of 146.95 W. This translated to a power per radiation area of 1967.80 W/m^2 and a power per mass of 464.22W/kg. As compared to the theoretical value for the radiation area the efficiency of the rectangular design is 18.3%. The raw numerical data obtained from FLUENT® used to determine the above values is provided in Table 19.

Table 19. Power values for heat pipe with ratio of 1.0 and no wick profile boundary condition.

Heat Pipe	**0.25 Ratio**	**Power (W)**
End Cap		-0.3925079
Fins		-80.260336
Insertion Tube		144.89731
Pipe Interior		0
Outer Radiation Surface of Pipe		-66.300562
Net		-2.3417085
Error	2.243800307	%

The temperature profile of the heat pipe is shown in Figure 41. The insertion tube temperature is held at 700 K and the end temperature is 409 K. The temperature drops by 220 K along the majority of the heat pipe.

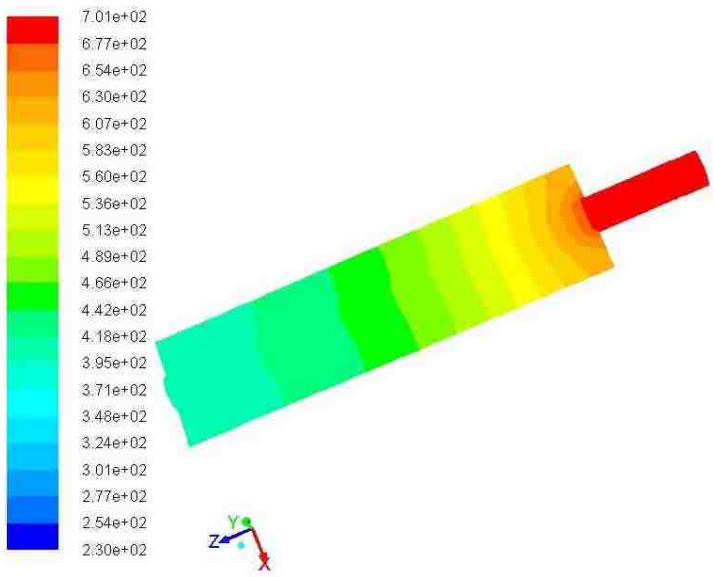

Figure 41. Temperature (K) profile of heat pipe with 1.0 ratio and no wick profile boundary condition.

5.4.6 Ratio of 1.25

The heat pipe geometry with fin length to diameter ratio of 1.25 had a power input of 155.22 W and an output of 160.50 W. The raw numerical data obtained from FLUENT® used to determine the above values is provided in Table 20. This translated to a power per radiation area of 2579.56 W/m^2 and a power per mass of 636.65 W/kg. As compared to the theoretical value for the radiation area the efficiency of the rectangular design is 23.4 %.

Table 20. Power values for heat pipe with ratio of 1.25 and no wick profile boundary condition.

Heat Pipe	**1.25 Ratio**	**Power (W)**
End Cap		-0.039151176
Fins		-95.579111
Insertion Tube		155.22203
Pipe Interior		0
Outer Radiation Surface of Pipe		-64.884426
Net		-5.280658176
Error	3.2900746	%

The temperature profile of the heat pipe is shown in Figure 42. The insertion tube temperature is held at 700 K and the end temperature is 407 K. The majority of the temperature drop occurs in the first third of the heat pipe. This leaves a large portion of the pipe and fin at a relatively low temperature.

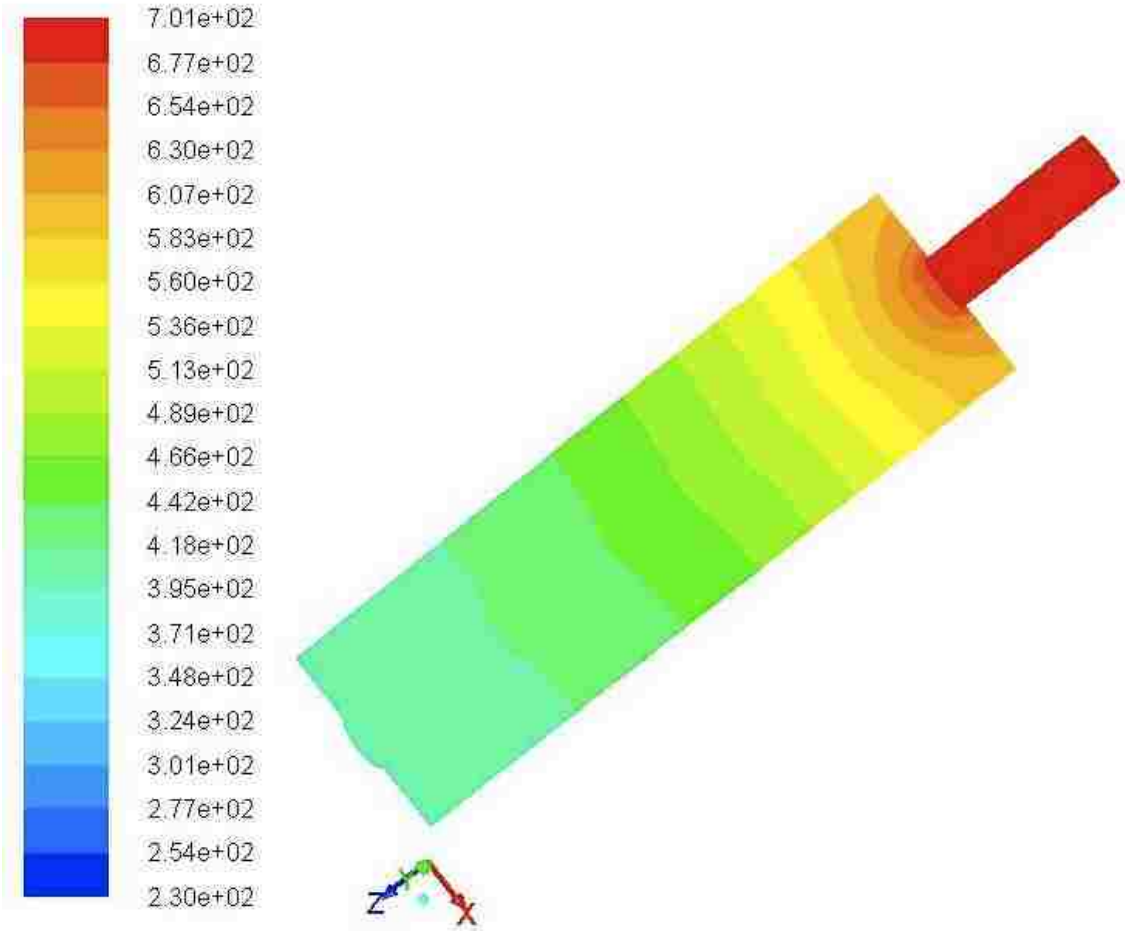

Figure 42. Temperature (K) profile of heat pipe with 1.25 ratio and no wick profile boundary condition.

5.4.7 Ratio of 1.5

The heat pipe geometry with fin length to diameter ratio of 1.50 had a power input of 164.0 W and an output of 169.84 W. This translated to a power per radiation area of 2434.28 W/m^2 and a power per mass of 621.21 W/kg. As compared to the theoretical value for the radiation area the efficiency of the rectangular design is 22.6 %. The raw numerical data obtained from FLUENT® used to determine the above values is provided in Table 21.

Table 21. Power values for heat pipe with ratio of 1.5 and no wick profile boundary condition.

Heat Pipe	**1.5 Ratio**	**Power (W)**
End Cap		-0.37258853
Fins		-107.08915
Insertion Tube		163.96104
Pipe Interior		0
Outer Radiation Surface of Pipe		-62.380008
Net		-5.88070653
Error	3.462462351	%

The temperature profile of the heat pipe is shown in Figure 43. The insertion tube temperature is held at 700 K and the end temperature is 402 K. The temperature drops 200 K in the first quarter of the heat pipe. This leaves the majority of the heat pipe operating at a lower temperature than other designs.

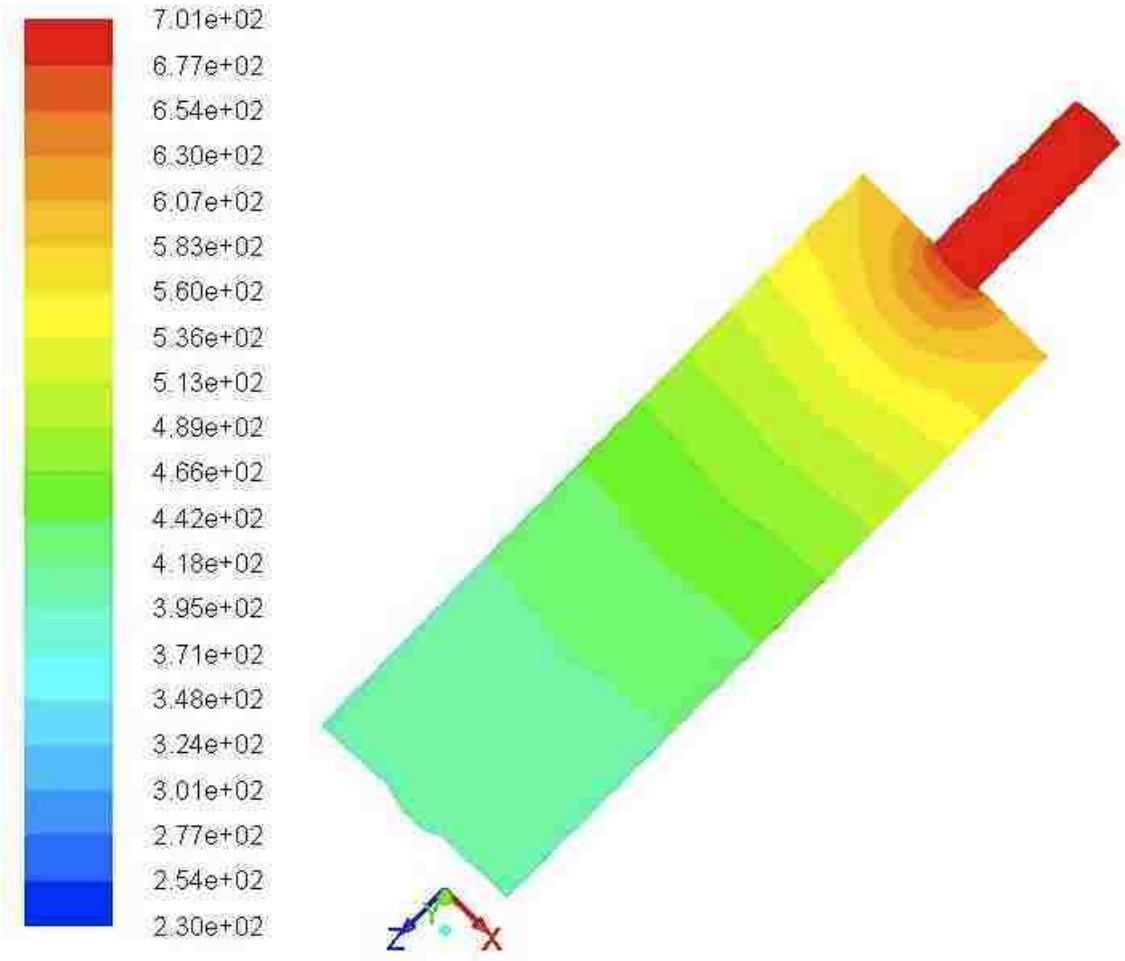

Figure 43. Temperature (K) profile of heat pipe with 1.5 ratio and no wick profile boundary condition.

5.4.8 Results and Discussions of Fin Length Comparison without Wick Profile Data

The following results shown in Figure 44 are the temperature contours of the simulations comparing fin ratios. From the contour plots it is observed that the temperature decreases more rapidly as the fin length is increased. This combined with the increase in mass due to general size demonstrates that a smaller fin length is reasonable and possibly preferable.

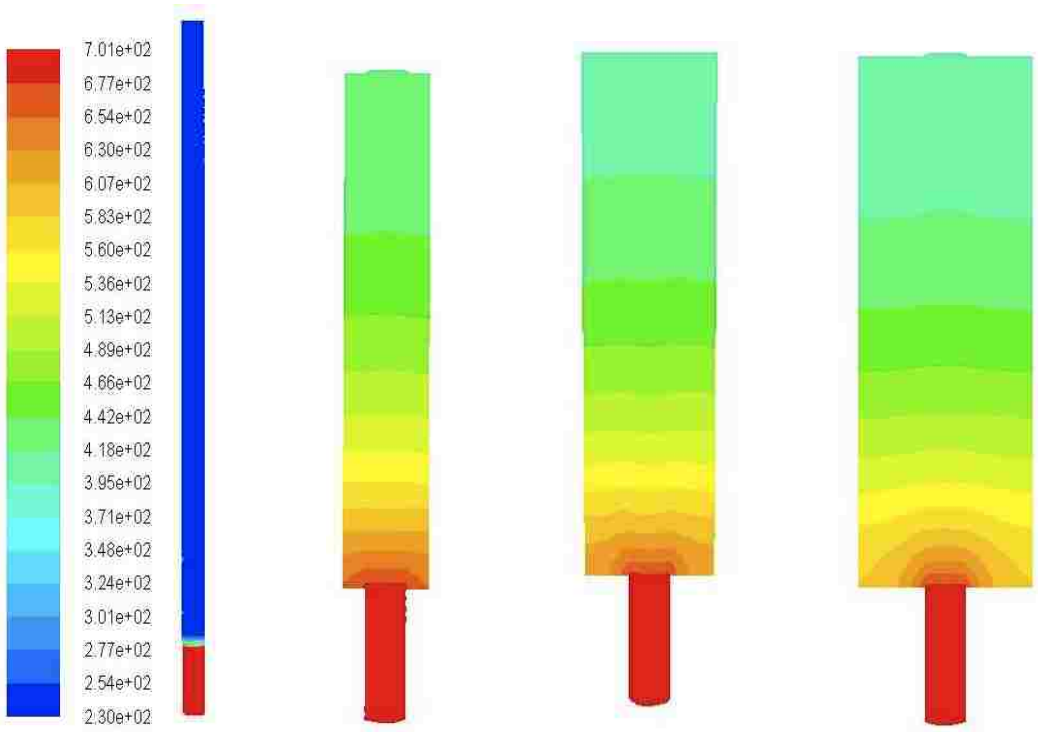

Figure 44. Temperature comparison of various fin widths and no wick profile boundary condition. (a) Heat Pipe (b) Heat Pipe with ratio of 0.5 (c) Heat Pipe with ratio of 1.0 and (d) Heat Pipe with ratio of 1.5

The following data in Table 22 shows that maximum heat transfer per unit area and per unit mass occurs at a fin width to pipe diameter of 0.5 ratio. It is also of note that the efficiency decreases as the width of the fins increase. This decrease in efficiency, approximately 7%, is negligible and thus not a primary concern in determining the best fin width to pipe length ratio.

Table 22. Comparison of power per unit area and power per unit mass for various fin width to pipe diameter for designs with no wick profile boundary condition.

Ratio	Output	Area	Mass	Power/Area	Power/Mass	Theoretical Power Output	Efficiency
	W	m^2	kg	W/m^2	W/kg	W	%
0	1.24	0.05374	0.9476	23.07	1.31	578.487973	0.21435191
0.25	104.36	0.03199	0.1704	3262.27	612.44	344.358583	30.305619
0.5	168.09	0.03956	0.1884	4248.99	892.20	425.846375	39.4719809
0.75	137.3	0.04681	0.2088	2933.13	657.57	503.889505	27.2480372
1	107.56	0.05466	0.2317	1967.80	464.22	588.391377	18.2803495
1.25	160.5	0.06222	0.2521	2579.56	636.65	669.771523	23.9633956
1.5	169.84	0.06977	0.2734	2434.28	621.21	751.044024	22.6138541

The power per unit area and the power per unit mass were graphed as shown in Figure 45. The graph shows that the power output per unit mass is maximized at a fin ratio of 0.5. This would indicate that the optimal fin ratio is 0.5 due to this being overall maximum for both power parameters. This is substantiated in bar graphs of the power per unit radiation area, Figure 46, and the power per unit mass, Figure 47.

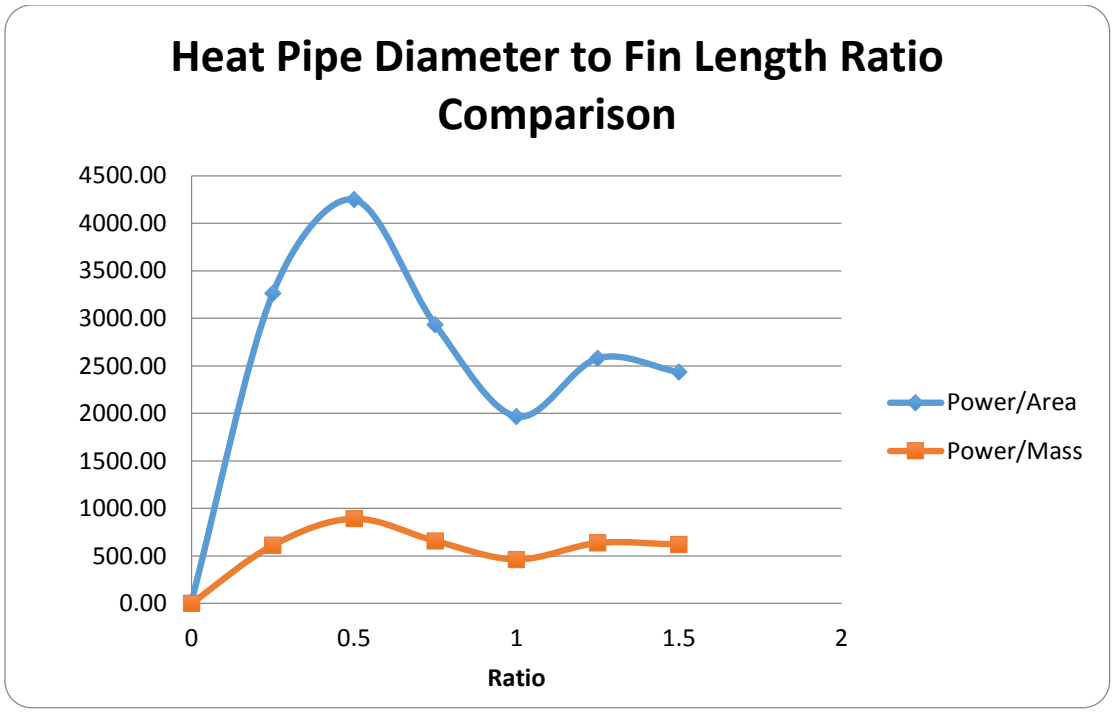

Figure 45. Comparison of power per unit area and power per unit mass for various fin width to pipe diameter for designs with no wick profile boundary condition.

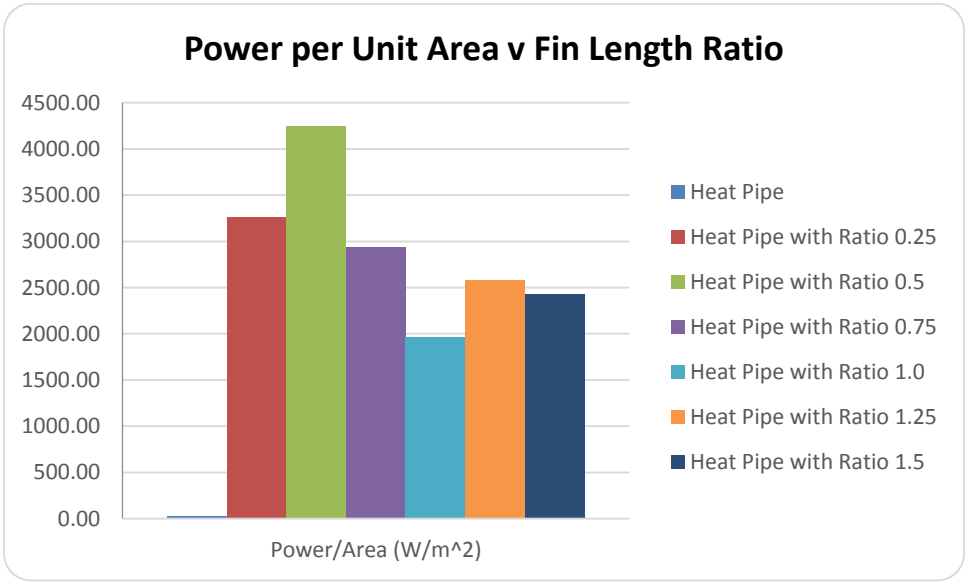

Figure 46. Power per unit area for various fin ratios for design with no wick profile boundary condition.

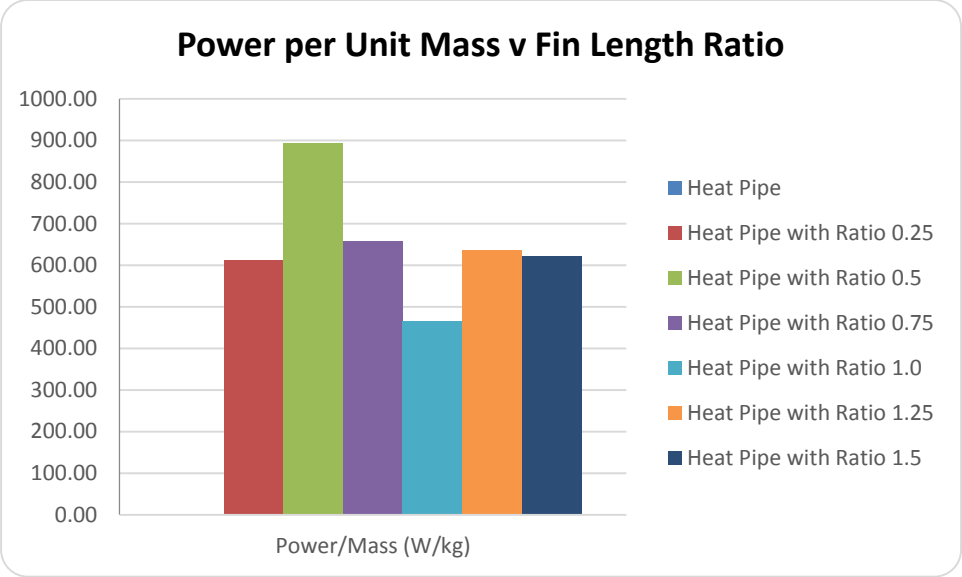

Figure 47. Power per unit mass comparison for various fin ratios for with no wick profile boundary condition.

5.5 Comparison of Non-Wick Effect Trials and Wick Effect Trials

The temperature of the exterior of each heat pipe was exported into Excel. Using Excel, the axial external heat pipe temperature was plotted and compared to the expected profile for both the wick performance study and the benchmark study. The results of this analysis are shown below.

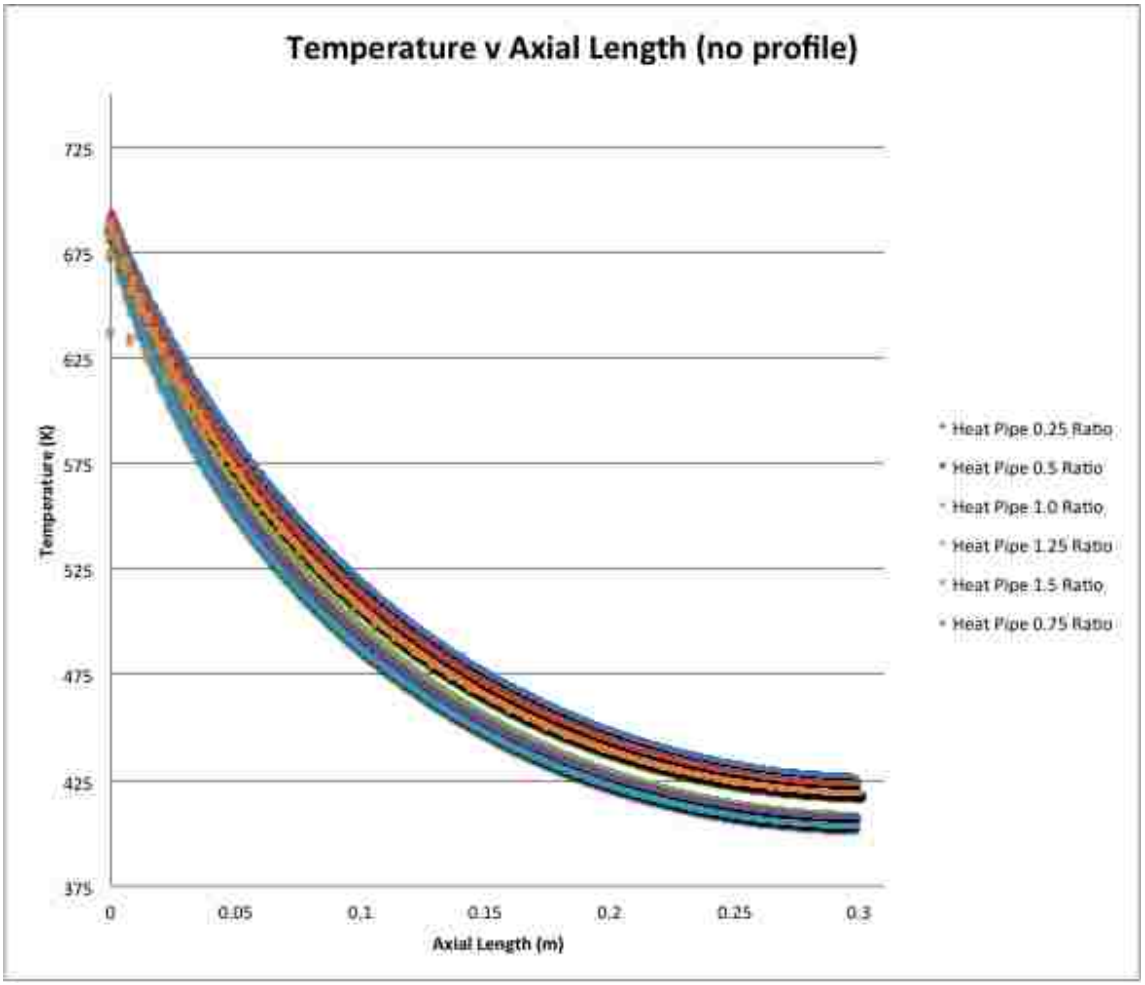

Figure 48. Comparison of power per unit area and power per unit mass for various fin width to pipe diameter with no interior temperature profile.

The het pipe temperature profiles represented in Figure 48 were determined to be lacking because of the failure to take internal wick effects into consideration in the model. The temperature profile drops quickly, similar to that of the solid geometries, since all the effects are those of conduction and radiation. For this reason the pipe interior was modeled with a simulated wick performance. This boundary condition takes into account the convection that occurs in the working fluid. In doing this, the efficiency increases to that of the Juhasz's (1998) design. The temperature profile also changes to mimic that of the flight test data found in Chapter 4. By including the interior fluid effects the operating

temperature along the heat pipe is increased to a steady temperature around 600K. The external heat pipe temperatures using the wick profile information are provided below in Figure 49. These are consistent with both the wick study and the flight test data.

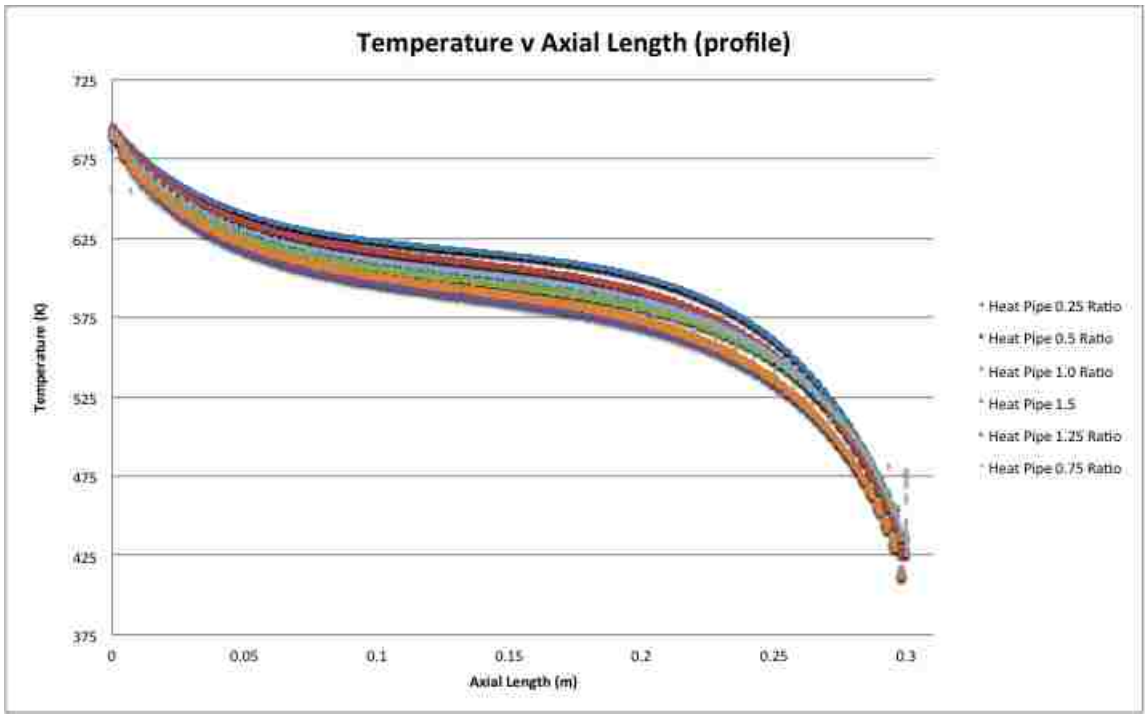

Figure 49. Comparison of power per unit area and power per unit mass for various fin width to pipe diameter with an interior temperature profile.

Chapter 6
Conclusions

A series of various geometries of solid fins and heat pipes with and without fins were modeled using FLUENT. The general heat pipe design consisted of a heat pipe with a 25 mm outer diameter, 23 mm inner diameter, and was 300 mm in length. Fin sizes ranged from 6.25 mm to 37.5 mm in length. Using the power output per unit area and power output per unit mass, to verify that a heat pipe was the best selection for a lunar radiator system.

- The parametric study returned the expected results that the heat pipe provided the highest power output for both the mass and radiation area. The heat pipe design is superior to the solid geometries that were considered. The heat pipe was lighter and had the same radiation area. The heat pipe was able to radiate more heat that it's solid counterparts as well.
- The heat pipe with integrated fin design outperformed the standard heat pipe. The fin allowed the length to be decreased by over half and also reduced the mass of the pipe. It also provided higher power transfer out of the system.
- The heat pipe with a fin ratio of 0.5, 12.5 mm, was the best performing design when the effect of the wick was not taken into account. It produced the highest power output for both mass and area. However, this did not accurately describe the realistic operation of the heat pipe.
- The heat pipe with a fin ratio of 0.5 was the best performer when the wick profile was applied. The 0.25 fin ratio design provided better efficiency and heat transfer per unit area; however, the 0.5 fin ratio performed nearly as well and had a slight

advantage in the power output per unit mass. This improved performance, 34.47 W/kg, could translate into nearly 5 kW increase for a radiator system containing 138 finned heat pipes. This coupled with the reduced mass, a major consideration for space systems, drove the decision to select the 0.5 fin ratio as the optimal design.

APPENDIX

NOMENCLATURE

A – area (m^2)

A_{rad} – radiation area (m^2)

ε - emissivity

h – convective heat transfer coefficient ($W/m^2 \cdot K$)

k – thermal conductivity ($W/m \cdot K$)

q – heat flux per unit area (W/m^2)

n - efficiency

Q_{calc} – heat flux calculated using Fluent design (W)

Q_{ideal} – heat flux for an ideal system (W)

Q_{real} – heat flux for a real system (W)

Q_{theo} – heat flux calculated using theoretical real equation (W)

σ – Stefan-Boltzman constant ($W/m^2 \cdot K$)

T – temperature (K)

T_{in} – temperature of system input (K)

T_{sink} – temperature of ambient environment (K)

x – length (m)

ρ – density (kg/m^3)

ν – velocity (m/s)

τ – shear stress ($kg/ m \cdot s^2$)

E – energy (kJ)

k_{eff} – effective conductivity ($W/m \cdot K$)

J_j - diffusion flux ($kg/m^2 \cdot s$)

p- pressure (Pa)

h – sensible enthalpy (kJ/kg)

Y_j- mass fraction the component that is in the gas form

c_p – specific heat at constant pressure (kJ/kg·K)

S_h – energy added by chemical reaction and other volumetric heat sources (kJ)

S_m – mass added to the continuous phase from the dispersed second phase (kg)

g –gravity (m/s^2)

F – external force ($kg \cdot m/s^2$)

References

1. Antoniak, Z.I., Webb, B. J., and Bates, J. M., 1991, "Testing of Advanced Ceramic Fabric Heat Pipe for a Stirling Engine," AIAA/NASA/OAI Conference on Advanced SEI Technologies, Cleveland, Ohio.
2. Arslanturk , C., 2005, "Optimum Design of Space Radiators with Temperature-Dependent Thermal Conductivity," Applied Thermal Engineering 26 (1149–1157)
3. Belvin, W.K., Watson, J.J., and Singhal, S.N., 2006, "Structural Concepts and Materials for Lunar Exploration Habitats," American Institute of Aeronautics and Astronautics, Space 2006, San Jose, CA.
4. Bowman, W.J., and Maynes, D., 2001, "Comparaison of Standard and Heat-Pipe Fins with Specified Tip Temperature Condition," Journal of Thermophysics and Heat Transfer Vol.15 No.4 (421-426), doi: 10.2514/2.6645
5. Bowman, W. J., Moss, T. W., Maynes, D., and Paulson, K. A., 1999, "Efficiency of a Constant-Area, Adiabatic Tip, Heat Pipe Fin," J. Thermophysics, Vol. 14, No. 1:Technical Notes (112-115), doi: 10.2514/2.6497
6. Bowman, W.J., Storey, J.K. and Svensson, K.I., 1999, "Analytical Comparison of Constant Area, Adiabatic Tip, Standard Fins, and Heat Pipe Fins," Journal of Thermophysics and Heat Transfer Vol.13 No.2 (269-272), doi: 10.2514/2.6432
7. Brandhorst , H.W. and Rodiek, J.A., 2006, "A Liquid Sheet Radiator for a Lunar Stirling Power System," Space Research Institute, Auburn University, Auburn University, AL 36849-5320
8. Diwekar, U.M. and Morel, B., 1993, "Space Nuclear Power Plants – I," Computers and Chemical Engineering, Vol. 17 No.9, pp 873-878
9. Elliott, J.O., Lipinski, R.J., And Poston, D.I., 2003, "Design Concept for a Nuclear Reactor-Powered Mars Rover," Space Technology and Application International Forum (STAIF 2003) Albuquerque, NM, USA
10. Faghri, Amir, 1995, *Heat Pipe Science And Technology*. Taylor & Francis Group. ISBN 978-1560323839
11. Ganapathi, G.B., Birur, G.C., Tsuyuki, G.T., McGrath, P.L. and Patzold, J.D., 2003, "Active Heat Rejection System on Mars Exploration Rover - Design Changes from Mars Pathfinder," AIP Conf. Proc., Volume 654, pp. 206-217
12. Incropera, F.P. and DeWitt, D.P., 1996, *Fundamentals of Heat and Mass Transfer*, John Wiley & Sons, Inc. 4th edition (110-130 and 634-754)
13. Juhasz, A.J., 1998, "Design Considerations for Lightweight Space Radiators Based on Fabrication and Test Experience With a Carbon-Carbon Composite Prototype Heat Pipe," National Aeronautics and Space Administration, Glenn Research Center, Cleveland, Ohio 44135
14. Juhasz, A.J., 2001, "Mathematical Analysis of Space Radiator Segmenting for Increased Reliability and Reduced Mass," National Aeronautics and Space Administration, Glenn Research Center, Cleveland, Ohio 44135 http://ntrs.nasa.gov/archive/nasa/casi.ntrs.nasa.gov/20010069503_2001112709.pdf.
15. Juhasz, A.J., 2007, "Heat Transfer Analysis of a Closed Brayton Cycle Space Radiator.," National Aeronautics and Space Administration, Glenn Research Center, Cleveland, Ohio 44135

16. Juhasz, A.J., Tew, R.C., Thieme, L.G., 2000, "Parametric Study of Radiator Concepts for Stirling Radioisotope Power System Applicable to Deep Space Missions," National Aeronautics and Space Administration, Glenn Research Center, Cleveland, Ohio 44135
http://gltrs.grc.nasa.gov/reports/2000/TP-2000-209676.pdf.
17. Keddy
18. Klein, A.C., Al-Baroudi, H., Gulshan-Ara, Z., Kiestler, W.C., Snuggerud, R.D., Abdul-Hamid, S.A., and Marks, T.S., 1993, "Fabric Composite Radiators for Space Nuclear Power Applications. Final Report," Oregon State Univ., Corvallis, OR (United States). Dept. of Nuclear Engineering
DOI: 10.2172/106730
19. Krikkis, R.N. and Razelos, P., 2002, "Optimum Design of Spacecraft Radiators With Longitudinal Rectangular and Triangular Fins," Journal of Heat Transfer October 2002, Vol. 124 (805-811).
20. Krishnaprakas, C.K. and Narayana, K.B., 2003, "Heat transfer analysis of mutually irradiating fins," International Journal of Heat and Mass Transfer 46 (761–769), doi: 10.1016/S0017-9310(02)00356-3 .
21. Mattick, A.T. and Hertzberg, A., 1981, "Liquid Droplet Radiators for Heat Rejection in Space," Journal Energy, Vol. 5, No. 6**.**
22. Mattick, A.T. and Hertzberg, A., 1985, "Liquid Droplet Radiator Performance Studies," Acta Astronautica Vol. 12, No. 7/8, pp. 591-598
23. Naumann, R.J., 2004, "Optimizing the Design of Space Radiators," International Journal of Thermophysics, Vol. 25, No. 6
24. Nelson, G, 2007, "Liquid Droplet Space Radiator," University of California, San Deigo, MAE221A – Heat Transfer
25. Pfeiffer, S.L., 1989, "Conceptual Design of Liquid Droplet Radiator Shuttle-Attached Experiment," Grumman Space Systems, Bethpage, New York
26. Roy, S.K. and Avanic, B.L., 2006, "Optimization of a Space Radiator with Energy Storage." International Communications in Heat and Mass Transfer, Vol. 33 iss: 5
27. Ruess, F. Schaenzlin, J. and Benaroya, H., 2006, "Structural Design of a Lunar Habitat," Journal of Aerospace Engineering, Vol. 19 No. 3
28. Siamidis, J., 2006, "Heat Rejection Concepts for Lunar Fission Surface Power Applications," Analex Corporation, Brook Park, Ohio, NASA/CR—2006-214388
29. Tagliafico, L.A. and Fossa,, M., 1997, "Lightweight radiator optimization for heat rejection in space," Heat and Mass Transfer 32 (239–244)
30. Tagliafico, L.A. and Fossa,, M., 1999, "Liquid Sheet Radiators for Space Power Systems," Proceedings of the Institution of Mechanical Engineers. Part G, Journal of aerospace engineering [0954-4100] vol: 213 iss:6 pg:399 -406
DOI: 10.1243/0954410991533115
31. Teti, N., 2002, "Carbon-Carbon Radiator Validation Report", Swales Aerospace, Beltsville, Maryland 20705
http://eo1.gsfc.nasa.gov/new/validationreport/Technology/Documents/Reports/CCR.pdf
32. Vaughn, W., Shinn, E., Rawal, S., and Wright, J., 1998, "Carbon-Carbon Composite Radiator Development for the EO-1 Spacecraft", Technical Report, NASA Langley Technical Report Server

http://www.acm-nevada.com/Technical/Radiator%20C-C.pdf
33. Woloshun, K.A. Merrigan, M.A., Sena, J.T., Secary, J., “High Temperature Heat Pipe Experiments Aboard the Space Shuttle.” AIP Conf. Proc. 271, pp. 523-531

VITA

Graduate College
University of Nevada, Las Vegas

Virginia Ruth Bieger

Local Address:
10146 Ragdoll Ave.
Las Vegas, Nevada 89166

Degree:
Bachelor of Science, Chemical Engineering
Louisiana Tech University

Publications:

Virginia R. Bieger, Jian Ma, Investigation of Lightweight Space Radiator Design for Low and No Gravity Environments, Proceedings of the ASME 2011 International Mechanical Engineering Congress & Exposition, 2011, Denver, Colorado, USA, November 2011

Thesis Title:
Numerical Modeling of Heat Pipe Radiator

Thesis Examination Committee:
Chairperson: Yitung Chen. Ph.D.
Committee Member: Robert F. Boehm, Ph.D.
Committee Member: Hui Zhao, Ph.D.
Committee Member: Jian Ma, Ph.D.
Graduate Faculty Representative: Yingtao Jiang, Ph.D.